ALSEP CASK COOLING

FEASIBILITY STUDY

Prepared by B Nordquist
B. Nordquist

Approved by J L McNaughton
J. L. McNaughton

LIST OF FIGURES

LIST OF TABLES

LIST OF DRAWINGS

1.0 INTRODUCTION

1.1 Background

In June of 1967, NASA Headquarters held a review of the ALSEP Program as related to the overall Apollo mission safety. Specific attention was given to the safety aspects of the RTG fuel cask which maintains an on pad temperature of approximately 650°F. It was determined that such a temperature level would represent a potential ignition hazard to the vehicle propellant vapors. Therefore MSC requested that Bendix conduct a preliminary thermal study to determine the feasibility of reducing the graphite fuel cask surface temperature to a level below 400°F during the prelaunch operations.

The results of the thermal study were transmitted to MSC on June 27, 1968. The basic conclusion was that the surface temperature of the graphite cask could be maintained below 400°F if the cask were locally purged from a directed nozzle or orifice supplied with a cooling flow of 225 to 450 cfm, (17-35 lb/min) at 70°F.

As a consequence of this study, an RTG Cask/Ignition Source Committee was established with members from MSC, KSC, GAEC, Sandia, LeRC, and Bendix. The purpose of this committee was to evaluate the potential ignition source problem of the cask in the presence of the various vehicle fuel vapors and to establish the requirements for reducing the cask surface temperature in a manner consistent with existing flight hardware and KSC capability. The first meeting of the committee was held at MSC on August 10-11, 1968. As a result of that meeting, Bendix was directed to submit a proposal to MSC for the purpose of conducting an engineering feasibility study and development tests to maintain the graphite cask surface below a maximum temperature of 350°F. The study was initiated on August 15, 1967 and was completed on January 12, 1968. This report summarizes the analysis, design, and test activities conducted at Bendix during that period.

1.2 Review of Cask Cooling Requirements

The SNAP-27 graphite fuel cask (GLFC) is located to the left of the ALSEP compartment in the LM SEQ bay. At approximately T-16 hours in the Apollo launch sequence, the fuel capsule assembly (FCA) is loaded into the cask. This FCA has a thermal energy output of 1500 watts and a surface temperature of approximately 1100°F, at the time of loading. Upon loading, the GLFC surface temperature rises from ambient to a free convection level between 550° and 650°F in approximately one hour. After vehicle liftoff and the subsequent loss of the convection portion of cooling to the cask, the GLFC surface temperature further increases to the range of 700° - 800°F.

It has been estimated that the spontaneous ignition temperature (SIT) of the command module and service module RCS propellant, monomethyl hyarazine (MMH) is of the order of 380°F - while the other vehicle propellants, UDMH and N_2H_4, have spontaneous ignition temperatures of 480° and 518°F respectively. Because of the possibility of propellant leakage from the A/S or LM fuel disconnects, supply lines, or the tanks themselves, the cask assembly presents a potential ignition hazard to the vehicle.

In order to reduce this hazard, it is necessary to actively cool any exposed cask surfaces to a temperature level below that of the aforementioned spontaneous ignition temperatures.

1.3 Study Objectives

In order to guide the selection and evaluation of the various possible cask cooling systems, the following ground rules were established.

1. As a goal, the design approach should preserve current BxA/GE/GAEC flight interfaces in order to minimize the impact on existing design.

2. If possible, the implementation of the design should utilize existing KSC facility capabilities from both the ground and airborne systems.

3. Only on-pad cooling of the cask will be required.

4. The GE 19F graphite fuel cask design will be used for all thermal analysis and design

5. Only single fuel leakage failures will be accommodated.

In regard to implementing this cooling, several air/GN_2 vehicle purge systems are in existence in the vicinity of the cask or if deemed necessary, a water supply could be made available. Three basic cooling concepts were judged worthy of further study in regard to satisfying the above objectives. These concepts are listed below along with a brief summary of their system advantages, requirements, and constraints.

Concept I - Forced Convection, Air/GN_2 Cask Purge System

- Air/GN_2 supply is available from the S IV B instrumentation unit (IU) purge duct.
- Purge source located below nozzle yields simplest approach, with minimal impact to flight hardware.
- Implementation has the shortest lead time to hardware - and with lowest cost.
- Requirements include:

  1) Air/GN_2 flow rate of 20 to 50 lb/min

  2) Air/GN_2 supply pressure of 0.25 - 0.5 psig.

Concept II - Open and Closed Water Cooling Systems

- S IV B IU water/methanol system not recommended for supply source/per MSFC.
- Requirements include:

  1) Open system, flow rate of 4-5 lb/hr - closed system flow rate of 60 lb/hr for up to 60 hours.

  2) Overboard vent to avoid inside vapor problems.

  3) Mechanical disconnection of supply and removal of cooling system at liftoff.

  4) Monitor of water level.

  5) Additional modifications to ground supply, swing arm, unbilical plate, IU area, etc.

Concept III - Finned Graphite Fuel Cask

- Passive system with free convection cooling
- Requirements include:

1) 110 fins, 9 inches long, 0.1 inches thick, and 1.5 inches high
2) Removal of fins after vehicle launch
3) Total revision of the BxA/GE/GAEC/NAR interface including new cask support structure, etc.
4) Additional ALSEP weight of 5 lbs.

Based on the information presented to the RTG Cask/Ignition Source Committee in August 1967 at MSC, Bendix was directed to continue the cask cooling studies of Concepts I and II (Air/GN_2 purge and water jacket) and to suspend work on Concept III (Finned Cask).

1.4 Description of Selected Concepts

The scope of this study was to evaluate the feasibility of utilizing on-pad active cooling air and water systems to reduce the temperature of the external cask surface below 350°F. The BxA/GE/GAEC interface established in the ground rules of CCP #29 for the graphite fuel cask was used to define the envelope and mounting structure for the engineering models of the air/water cooling systems.

Some of the early conceptual cask cooling systems are shown in Figure 1.1. As indicated in Figure 1.1 from the standpoint of required mass flow and pressure differential, the fully enclosed systems present the most efficient means of cooling. However since the thermal dissipation from the cask is by pure radiation after the early portion of the launch sequence, it would be necessary to mechanically remove any enclosed cooling system after the GN_2 shutdown. Therefore the early phases of the study also included an investigation of the possible mechanisms of cooling shroud removal and/or destruction systems.

Because of the added complications and interference problems of the shrouded cooling systems, only the full axial shroud was actually fabricated for testing and the majority of testing was carried out with the various open flow configurations as pictured in Figure 1.2.

COMPARISON OF AIR/GN_2 PURGE SYSTEMS AND WATER SHROUD SYSTEMS
FOR ON PAD CASK COOLING CONFIGURATION

	AIR/GN_2 PURGE SYSTEMS				WATER SHROUD SYSTEMS	
	AXIAL FLOW			ENCLOSED FLOW	CLOSED	OPEN (BOILING)
	NOZZLE ATTACHED OPEN	NOZZLE ATTACHED SHROUDED	NOZZLE DETACHED			
	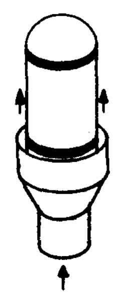	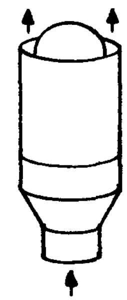	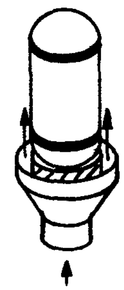	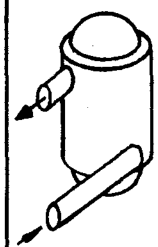	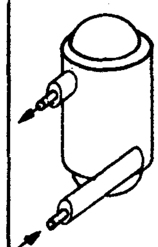	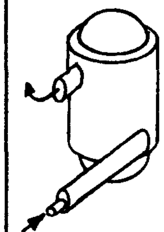
REQUIRED MASS FLOW RATE, #/MIN.	HIGH 35-50	MODERATE 20-40	HIGH 50	LOW 5-10	HIGH 60-80 (#/HR)	LOW 4-5 (#/HR)
REQUIRED PRESSURE DIFFERENTIAL, PSIG	1.0	0.4-0.8	1.0	0.1-0.3	3.0	5.0
DESIGN CONFIDENCE LEVEL	FAIR	GOOD	FAIR	GOOD	GOOD	GOOD
WEIGHT PENALTY	LOW	MODERATE	LOW	MODERATE	HIGH	HIGH
ON PAD CASK TEMPERATURE GRADIENTS	MODERATE	LOW	MODERATE	LOW	LOW	MODERATE
POST LAUNCH INTERFACE INTERFERENCES	LOW	HIGH	NONE	HIGH	HIGH	HIGH
MECHANICAL/THERMAL RELEASE SYSTEM REQUIRED	NO	YES	NO	YES	YES	YES

Figure 1.1 Early Cooling Concepts

	ATTACHED NOZZLE	ATTACHED PLUGGED NOZZLE	OPEN AXIAL FLOW	DETACHED PLUGGED NOZZLE	DETACHED NOZZLE AXIALFLOW	DETACHED NOZZLE 45° ANGLE	SHROUDED AXIAL FLOW
	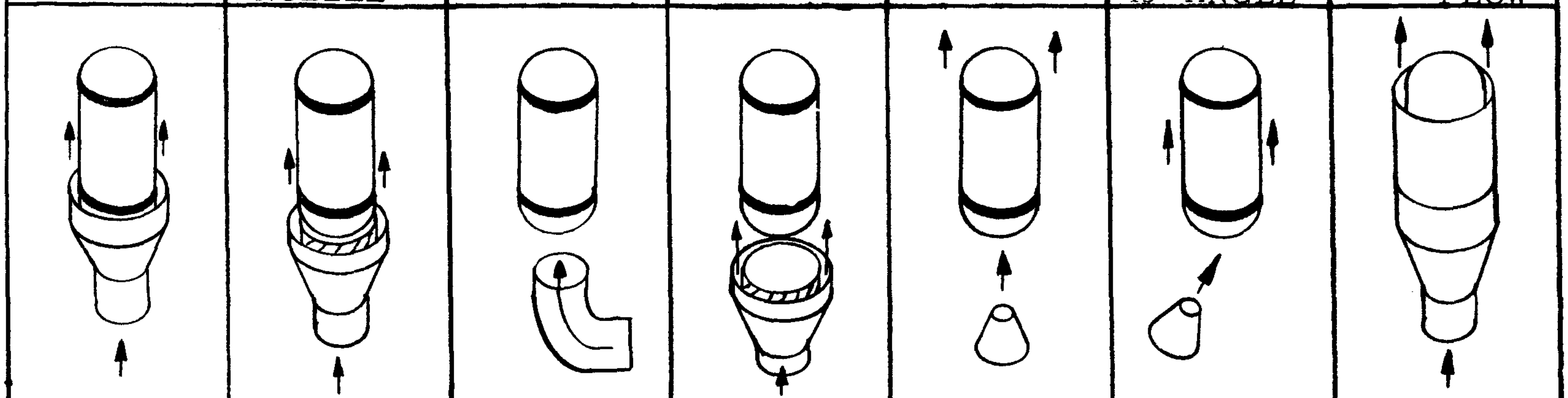						
Configuration Number	1	2	3	4	5	6	7

Figure 1.2 Schematic of Test Nozzle Configurations

In Section 2 a short synopsis of the test results is given and the actual test data is summarized. Then in Section 3 the analysis and correlation of this data is developed and in Section 4 the corresponding thermal model is discussed.

2.0 TEST RESULTS

A photograph of the actual test setup is shown in Figure 2.1, and the details of this unit are given in Section 2.3. The individual test runs are tabulated in Section 2.4 along with their pertinent flow parameters and resultant range of equilibrium temperatures.

2.1 Discussion of Data

Because the actual cask cooling was more efficient than had been predicted by the pre-test analysis, the test plan was modified midway through the testing of the attached plugged nozzle, (configuration 2 of Figure 1.2). This modification was instituted for two reasons. First, it was evident that all of the proposed systems and flow conditions would provide more than adequate cooling on the cask - and thus without a test plan modification, no data would be obtained in the marginal temperature range. Secondly, on the basis of early predictions the more remote nozzle locations had been discarded as providing inadequate cooling with the available flow conditions. However upon receiving the initial test results, it became apparent that this conclusion was not entirely valid.

The fact that the actual cask cooling was more effective than had been predicted was not a result of erroneous pre-test analysis. After reduction of the test data it was found that the measured values of the film coefficients were well above both the experimental and theoretical values which exist in the open literature. The actual reasons for this apparent discrepancy probably lie in the state of the boundary layer development and are discussed in Section 3.

Various detached nozzle configurations were thereupon tested in several axial positions below the cask. In addition it was found that the thermal shield on the inboard side of the cask would function as a leeward flow deflector so that the nozzles could also be placed outboard and at an angle with respect to the cask axis. Finally a fully shrouded axial flow configuration was tested for purposes of comparison with the pre-test analysis.

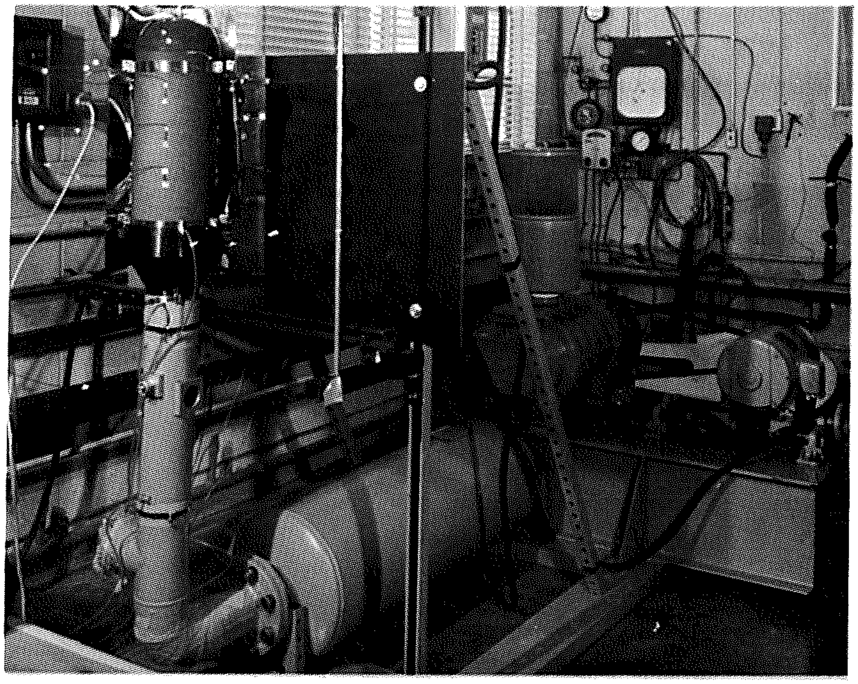

photo a

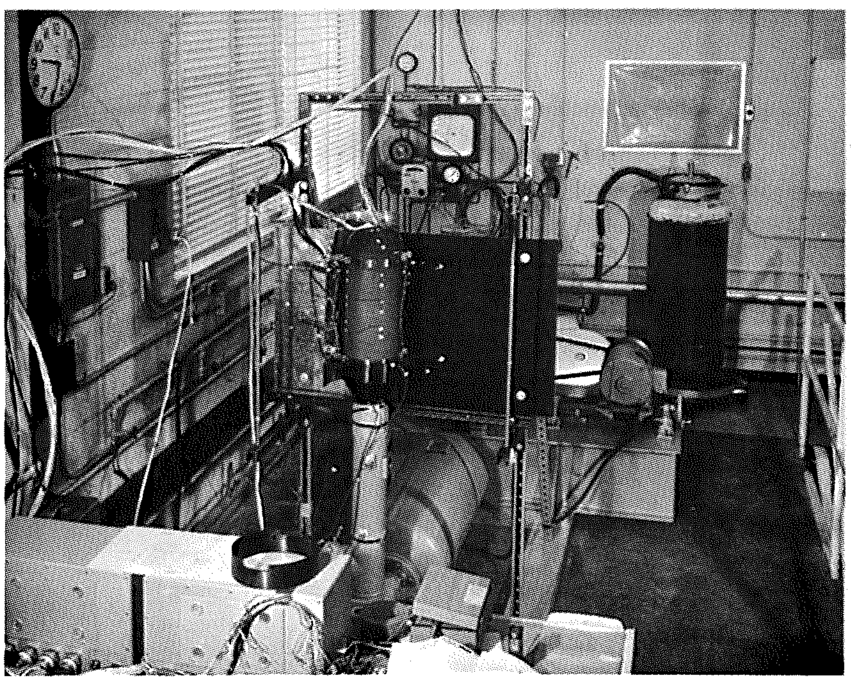

photo b

Figure 2.1 Test Setup for Cask Cooling Series

The velocity of the airflow was measured at each exposed thermocouple on the cask surface so that correlations of both the flow field and the film coefficients could be made. It was found that a good correlation could be achieved between the local velocity on the open side of the cask and the local cask surface temperature differential above that of ambient. To an acceptable experimental accuracy, this result may be written as

$$\frac{1}{\Delta T} = 9.5 \times 10^{-4} \, u_e^{\,0.71}$$

and is general for the open side of all but the shrouded cask. Upon coupling the above to the semi-empirical velocity correlations for open flow, the temperature differential may then be written as a function of the upstream flow conditions.

Basically the correlations for open flow cooling systems may be divided into two categories - one for the essentially two-dimensional flow from a plugged nozzle configuration and the other for the essentially three-dimensional flow from conical nozzles. Because of the geometric nature of the flow from a plugged nozzle, this type of cooling configuration is only useful when the nozzle is aligned with the cask axis. On the other hand, as long as the present thermal shield remains near the back side of the cask, it is possible to have an angle of as much as 45° between the axis of the conical nozzles and the cask axis. This thermal shield then acts to direct the flow up the back side of the cask.

As noted, the correlations themselves have been developed for the front (i. e., open side) of the cask where there is effectively no airflow interference from the structure, etc. They are given below as:

<u>Plugged Nozzle</u>

$$\Delta T = 62 \left[\frac{x + 1.9 \dfrac{\sqrt{\dot{m}}}{\Delta p^{1/4}}}{\left(\sqrt{\dot{m}} \;\; \Delta p^{1/4} \right)} \right]^{0.71}$$

Conical Nozzle

$$\Delta T = 48 \left[\frac{x + \dfrac{2.7 \sqrt{\dot{m}}}{\Delta p^{1/4}}}{\cos \theta \sqrt{\dot{m}}\, \Delta p^{1/4}} \right]^{0.71}$$

where

ΔT = temperature differential ~ °F

x = surface distance from nozzle to cask cylinder surface point ~ feet

m = mass flow ~ #/sec

Δp = pressure differential ~ psf

θ = angle between nozzle axis and cask axis.

These equations are plotted for a realistic range of input parameters in Figures 2.2 through 2.7.

Within a tolerance of several degrees, the actual maximum surface temperatures measured were invariably 10% higher than the maximum open side temperatures in °F. Thus from the ΔT of the correlations plus the ambient temperature, the maximum cask surface temperature may be predicted. Note also that the maximum ΔT will occur in the neighborhood of the maximum downstream distance on the thin-walled section of the cask cylinder.

Because of the presence of lightweight insulation on the structure above the cask, it is also of interest to note the cooling air velocities in this region. In Table I the range of velocities three feet above the cask are tabulated for the cooling configurations tested. These are quite low and their accompanying dynamic pressures are rather insignificant in terms of any damage which might be done by the cooling air.

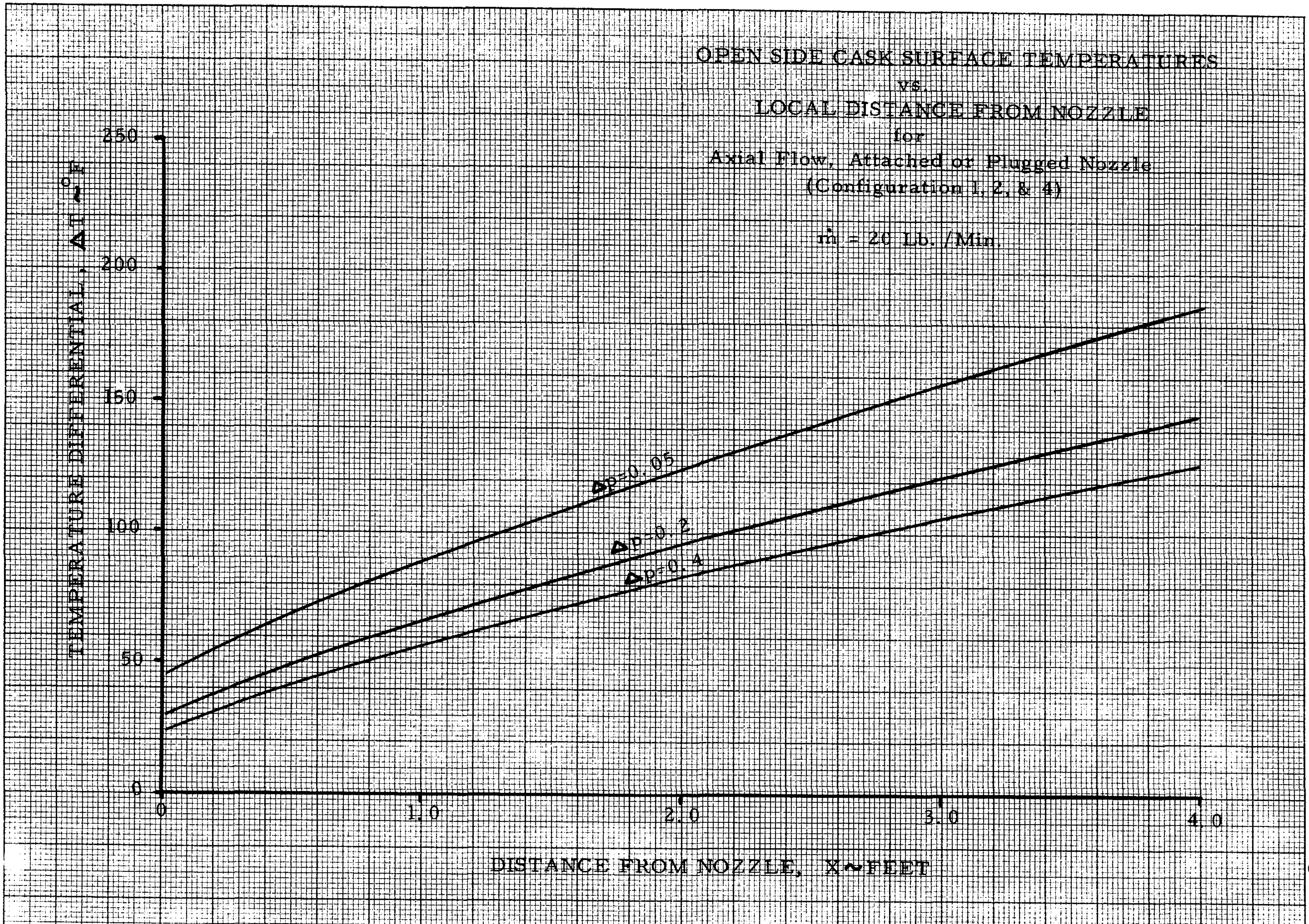
OPEN SIDE CASK SURFACE TEMPERATURES
vs.
LOCAL DISTANCE FROM NOZZLE
for
Axial Flow, Attached or Plugged Nozzle
(Configuration 1, 2, & 4)
ṁ = 20 Lb./Min.
TEMPERATURE DIFFERENTIAL, ΔT ~ °F
250
200
150
100
50
0
ΔP=0.05
ΔP=0.2
ΔP=0.4
0
1.0
2.0
3.0
4.0
DISTANCE FROM NOZZLE, X~FEET

Figure 2.2

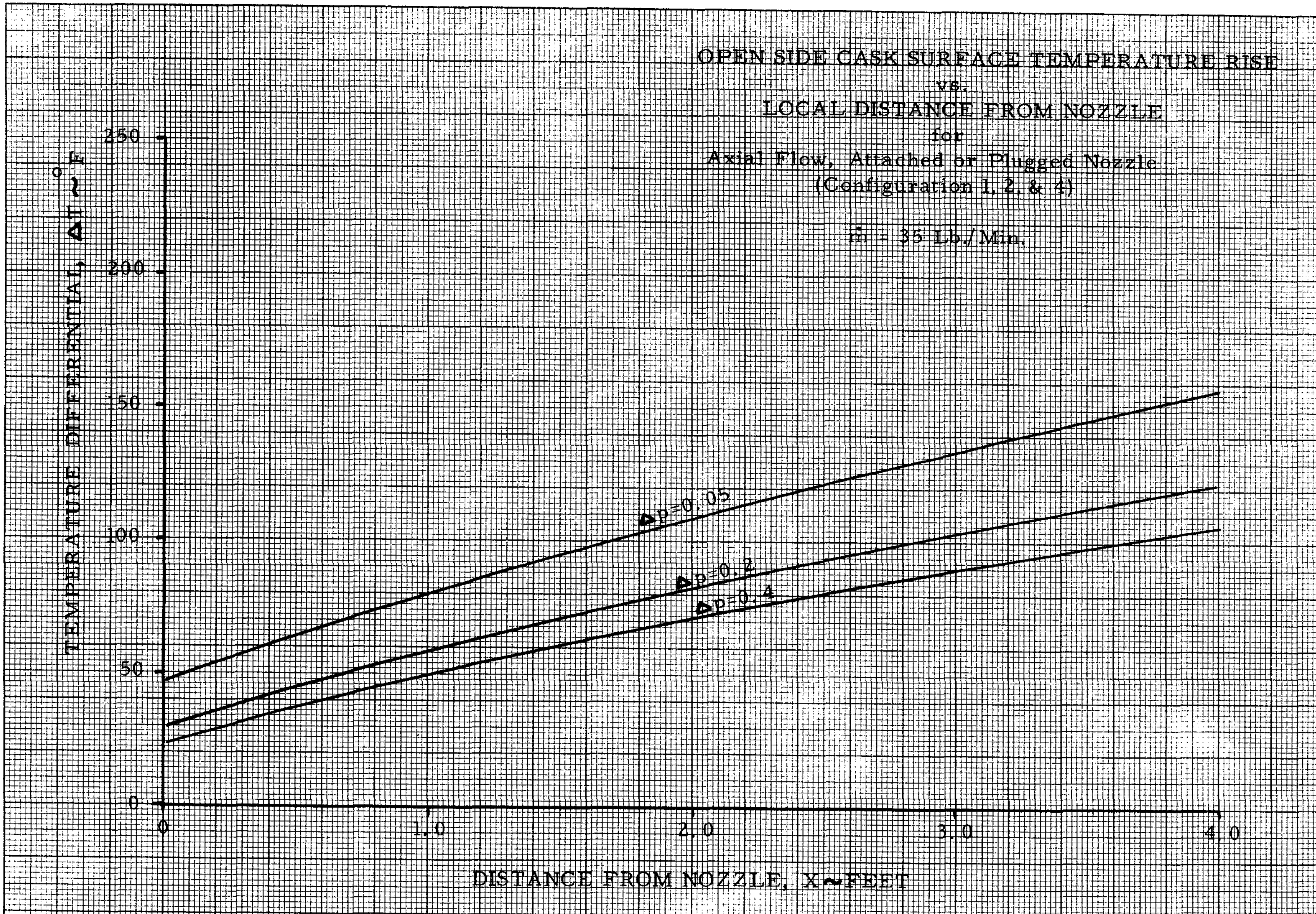
OPEN SIDE CASK SURFACE TEMPERATURE RISE
vs.
LOCAL DISTANCE FROM NOZZLE
for
Axial Flow, Attached or Plugged Nozzle
(Configuration 1, 2, & 4)
ṁ = 35 Lb./Min.
TEMPERATURE DIFFERENTIAL, ΔT ~ °F
250
200
150
100
50
0
1.0
2.0
3.0
4.0
Δp=0.05
Δp=0.2
Δp=0.4
DISTANCE FROM NOZZLE, X ~ FEET

Figure 2.3

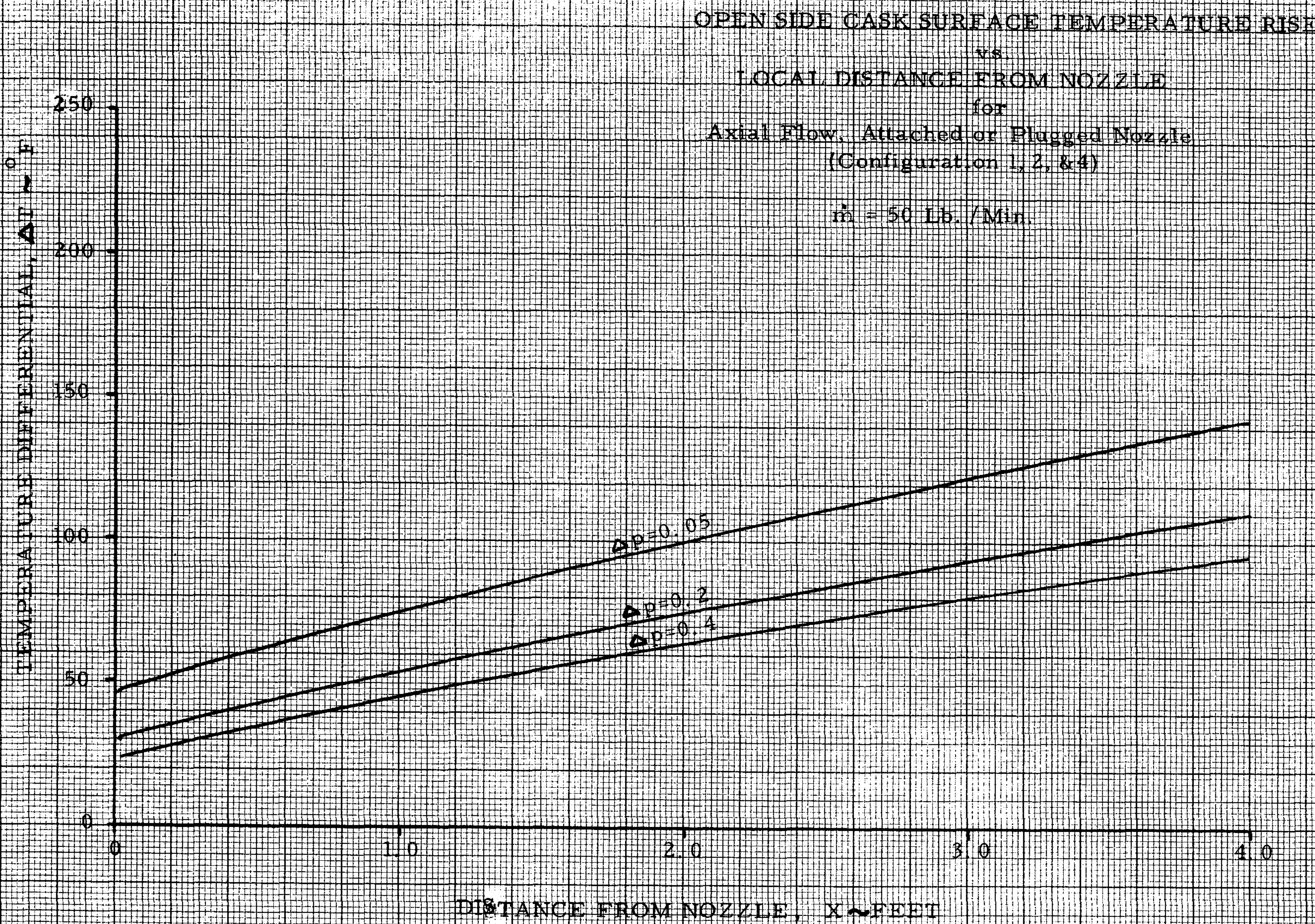
OPEN SIDE CASK SURFACE TEMPERATURE RISE
vs.
LOCAL DISTANCE FROM NOZZLE
for
Axial Flow, Attached or Plugged Nozzle
(Configuration 1, 2, & 4)
ṁ = 50 Lb./Min.
TEMPERATURE DIFFERENTIAL, ΔT ~ °F
250
200
150
100
50
0
0
1.0
2.0
3.0
4.0
DISTANCE FROM NOZZLE, X ~ FEET
Δp=0.05
Δp=0.2
Δp=0.4

Figure 2.4

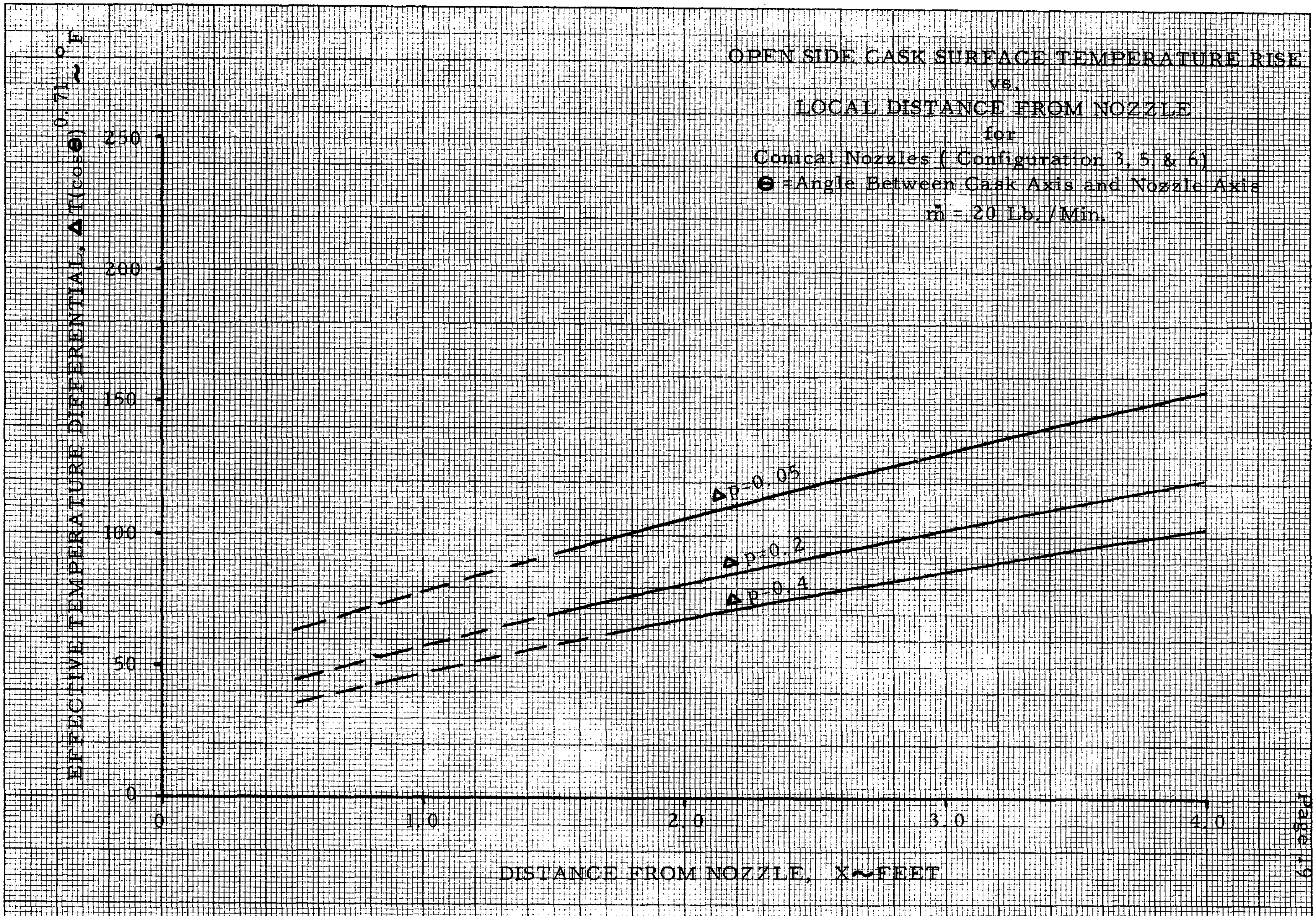
OPEN SIDE CASK SURFACE TEMPERATURE RISE
vs.
LOCAL DISTANCE FROM NOZZLE
for
Conical Nozzles (Configuration 3, 5, & 6)
θ =Angle Between Cask Axis and Nozzle Axis
ṁ = 20 Lb. /Min.
EFFECTIVE TEMPERATURE DIFFERENTIAL, ΔT(cos θ)^0.71 ~ °F
250
200
150
100
50
0
Δp=0.05
Δp=0.2
Δp=0.4
0
1.0
2.0
3.0
4.0
DISTANCE FROM NOZZLE, X~FEET

Figure 2.5

K+E 10 X 10 TO THE CENTIMETER 46 1513
18 X 25 CM. MADE IN U.S.A.
KEUFFEL & ESSER CO.

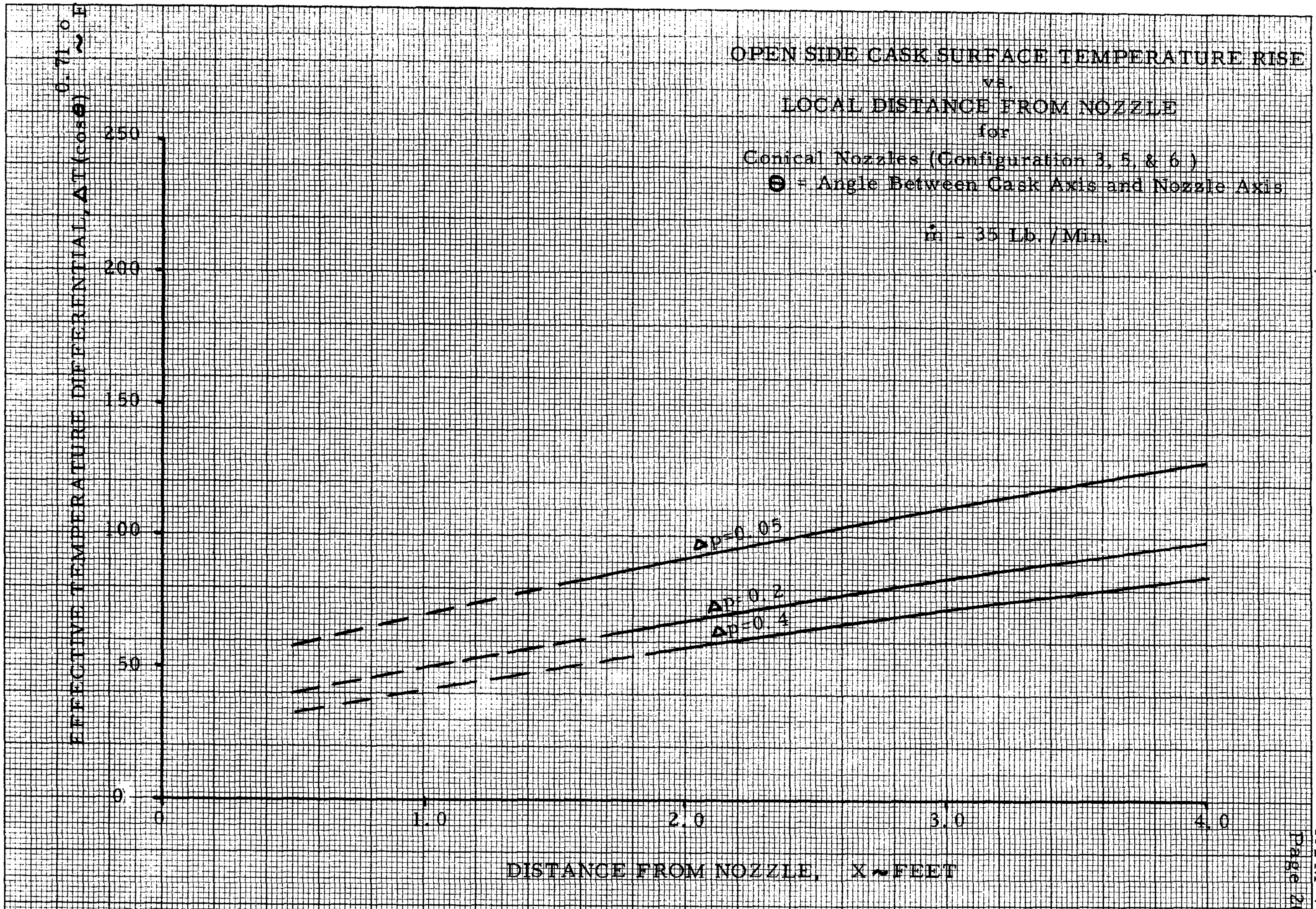

Figure 2.6

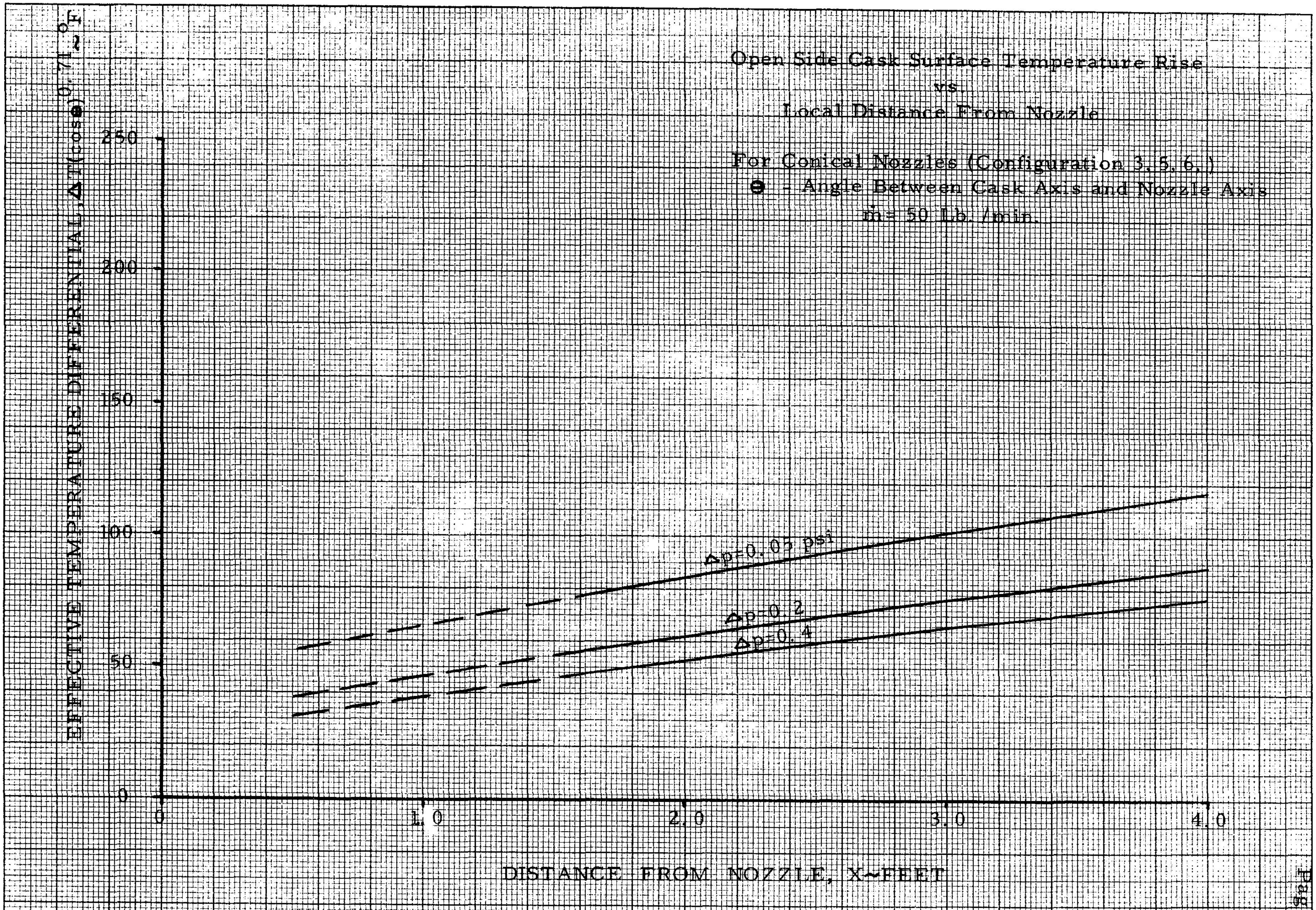
Open Side Cask Surface Temperature Rise
vs.
Local Distance From Nozzle
For Conical Nozzles (Configuration 3, 5, 6,)
⊖ - Angle Between Cask Axis and Nozzle Axis
ṁ = 50 Lb. /min.
EFFECTIVE TEMPERATURE DIFFERENTIAL, ΔT(cos⊖)^0.71 ~ °F
250
200
150
100
50
0
0
1.0
2.0
3.0
4.0
Δp=0.05 psi
Δp=0.2
Δp=0.4
DISTANCE FROM NOZZLE, X~FEET

Figure 2.7

TABLE I

TEST NOZZLE CONFIGURATIONS AND FLOW CONDITIONS

	ATTACHED NOZZLE	ATTACHED PLUGGED NOZZLE	OPEN AXIAL FLOW	DETACHED PLUGGED NOZZLE	DETACHED NOZZLE AXIALFLOW	DETACHED NOZZLE 45° ANGLE	SHROUDED AXIAL FLOW
	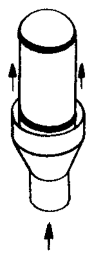	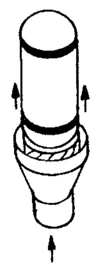	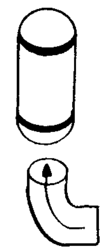	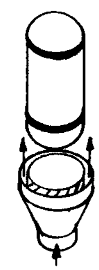	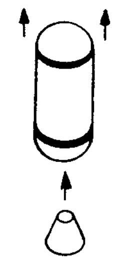	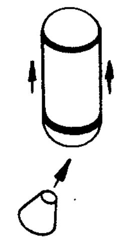	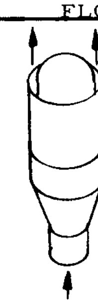
Configuration Number	1	2	3	4	5	6	7
Run Number	1 to 12	13 to 18 30 to 35	19 to 21	22 to 27	28 to 29	36 to 40	41 to 43
Range of Flow Conditions: Mass Flow #/min	4-50	10-50	24-53	18-35	22-35	18-43	5-20
Range of Flow Conditions: Pressures psi	.06-.83	.03-.42	.01-.05	.10-.33	.06-.13	.04-.56	.02-.19
Range of Flow Conditions: Nozzle Area in^2	2.80-8.40	3.56-9.16	19.6	3.56-7.8	8.95	3.14-19.6	5.17

Typical Flow Conditions to Maintain a Maximum Cask Wall Temperature of 200°F (using 70°F cooling air)

Flow Rate, #/min	15	25	50	35	30	30	8
Pressure Differential, psi	0.04	0.06	0.05	0.09	0.15	0.25	0.06
Maximum Velocity 3 feet above cask, fps	7	10	18	10	8	9	3

2.2 Recommendations

Under current planning it appears that the actual air supply for the cask cooling would be obtained from the IU cooling duct which presently exists in the vicinity of the cask. It has been estimated that the ductwork could supply approximately 35 lb/min of air at a pressure on the order of 0.3 psi. However the air supply temperature may be as high as 130°F as opposed to the 70°F of this test.

Since the maximum cask surface temperature is approximately ten percent higher than the maximum open side cask temperature, the maintenance of a maximum surface temperature of 350°F with an air supply temperature of 130°F would require a maximum correlated ΔT of 200°. As can be seen in Figures 2.2 through 2.7, this ΔT is well within the capability of the estimated air supply - irrespective of the particular cooling system configuration. However it should be noted that the current cask support hardware is now much more extensive than the original simulated test support structure. Therefore a wider margin (lower ΔT) will undoubtedly be required of the prototype configuration. Nevertheless, there will be a considerable latitude in the placement of the cooling nozzle in the flight vehicle. This latitude may thereby be used to advantage in terms of minimizing interference and revision problems in the existing hardware.

At present the IU duct consists of two deadend semicircles. For the cask cooling it had been proposed that these be joined by a "T" and that a second duct be routed from there to the cooling nozzle. However this modification appears to be an unwarranted complication since the location of this T is a considerable distance from the cask. A more simple solution would be to tap in to the IU duct at a location adjacent to the cask itself and merely connect the ends of the IU duct. The pressure drop in the duct itself is essentially negligible - regardless of the placement of the existing cooling holes and proposed nozzle. Therefore there would be no effective flow output change from the IU duct, whether the cask cooling air were taken from an asymmetrical point in the air supply system or not. However there would be a weight and interference saving if the IU tap were as close to the cask cooling nozzle as possible.

2.3 Test Setup

A photograph for the basic accessory hardware is shown in Figure 2. b. A variable speed drive was attached to the Roots blower so that the mass flow of air could be regulated from approximately twenty to fifty pounds per minute. A scrubber was attached to the output of the Roots blower in order to reduce the pulsation of the flow out of the blower. Ambient air at approximately 70°F was used in all tests and the air temperature rise across the blower for these operating conditions was essentially negligible.

The diagrams of the test plan nozzles are shown in Drawings 2, 3 and 4. However as noted in section 2. 1, the test plan was modified in the course of testing and conical nozzles of 3-3/8, 2-1/2, and 2-inch diameters were fabricated on location for additional testing. Also it was part of the test plan modification to operate the plugged nozzles fully separated from the cask and to operate the ducting as a cooling source without any nozzle.

The thermocouples for these tests were placed on the cask, electric fuel capsule, and associated support hardware as shown in Drawings 6 through 9. The static pressure for the air cooling system was measured along the supply duct as well as at the nozzle orifice by means of Statham pressure transducers. Also a thermocouple was placed in the downstream end of the air supply duct. The output of these sensors was monitored by an EI Data Acquisition System connected to the thermocouples and transducers through RIC reference boxes. A Sorenson 15 Kw power supply was used to power the Electric Fuel Capsule Simulator and this output was also monitored through the DAS system.

Additional on-site, hand operated instrumentation consisted of an Alnor Velometer and Thermocon. The velometer was used to measure the air flow velocities at the nozzle orifice, adjacent to the cask surface thermocouples, above the cask, etc. for the purposes of overall test correlations. The thermocon was used to check the surface temperatures on non-instrumented areas of the cask.

2.4 Summary of Test Data

The test nozzle configurations and flow conditions are given in Table I. The individual runs are tabulated in Table II with nozzle sizes given below.

Config. No.	Nozzle Area (in^2)
1a	8.40
1b	7.04
1c	5.17
1d	2.80
2a	9.16
2b	7.80
2c	5.92
2d	3.56
7b	5.17

The individual equilibrium temperatures are listed in Table III.

TABLE II

SUMMARY OF TEST DATA

Run Number	Configuration	Mass Flow #/min	Pressure Differential, psi.	Nozzle Exhaust Velocity ~ fps	Range of Surface Temperature
1	1a	39	0.18	143	103-146°F
2	1a	24	0.06	81	117-182
3	1a	50	0.30	191	93-129
4	1b	22	0.10	97	110-154
5	1b	35	0.22	145	98-128
6	1b	50	0.43	228	92-120
7	1c	15	0.10	93	118-159
8	1c	20	0.14	117	111-145
9	1c	30	0.29	160	100-129
10	1d	9	0.14	92	127-188
10a	1d	3.5	0.06	40	159-233
11	1d	20	0.41	212	104-140
12	1d	30	0.83	317	96-126
13	2a	22	0.05	78	121-201
14	2a	35	0.11	115	103-166
15	2a	50	0.22	163	96-148
16	2b	22	0.07	83	119-197
17	2b	35	0.14	127	101-163
18	2b	10	0.03	42	159-259
19	5" elbow	38	0.03	61	123-224
20	31" elbow	53	0.05	85	109-195
21	cask (3)	24	0.01	38	157-277
22	2b on	23	0.10	93	142-254
23	5" elbow (4)	35	0.16	139	115-206
24	2c on	35	0.30	190	112-196
25	5" elbow (4)	22	0.13	125	134-237
26	2d on	22	0.33	200	130-226
27	5" elbow (4)	18	0.23	167	143-246
28	3.4" diameter	22	0.06	75	132-231
29	nozzle on	35	0.13	120	109-189
	5" elbow (5)				
30	2c	21	0.10	102	132-192
31	2c	30	0.19	137	122-166
32	2c	11	0.03	57	161-246
33	2d	20	0.28	162	126-188
34	2d	34	0.42	208	116-164
35	2d	11	0.10	98	157-227

Run Number	Configuration	Mass Flow #/min	Pressure Differential, psi.	Nozzle Exhaust Velocity ~ fps	Range of Surface Temperature
36	5" nozzle, 14" off, cask (a) (b)	43	0.04	69	136-222°F
37	2.5" nozzle 45" off cask (a) 45° (b)	21	0.18	135	136-234
38		35	0.44	224	114-191
39	20" nozzle 45" off cask (a) 45° (b)	18	0.24	178	129-232
40		24	0.56	238	111-190
41	7b	20	0.19	94	113-146
42	7b	10	0.09	63	131-177
43	7b	4.6	0.02	28	177-264

TABLE III EQUILIBRIUM TEMPERATURES

Thermocouple number versus run number and location

RUN		THER SHLD	CASK SUPPORT BANDS								SPT STRK	LM STRUT	LM	CASK UPPER DOME				CASK EXTERNAL SURFACE											CASK INTERNAL SURFACE										EFCS LATCH PLT		EFCS SURFACE							
	TIME	1-13	14	15	16	17	18	19	20	21	22-35	36-43	44-53	54	55	56	57	58	59	60	61	63	64	65	66	67	68	69	70	71	72	73	74	75	76	77	78	79	80	81	82	83	84	85	86	87	88	89
1	11-15-67 2230	70-76	126	97	132	102	134	78	132	88	70-75	70-71	70-72	122	108	115	115	103	143	123	146	136	119	137	104	132	117	121	187	169	229	199	185	178	156	298	183	195	345	333	960	958	967	976	957	952	872	869
2	2340	69-77	153	113	160	117	164	78	162	98	70-74	70-71	70-72	127	117	132	131	137	175	149	182	169	143	168	124	157	138	144	219	200	267	234	220	211	184	327	205	218	365	354	977	973	981	992	967	965	887	882
3	11-16-67 0030	69-77	114	95	119	99	119	81	97	87	70-76	70-71	70-71	119	104	107	108	93	124	111	129	122	108	123	96	123	108	114	167	154	206	185	169	166	150	287	171	189	317	318	943	946	951	970	951	948	859	859
4	0245	68-75	133	100	143	107	144	78	140	92	69-73	69-70	69-70	139	122	127	125	122	150	133	154	148	124	150	110	143	124	132	188	169	229	202	195	187	193	312	200	221	324	300	946	935	959	958	949	950	874	872
5	0345	68-75	112	93	118	99	121	79	96	87	69-74	69-70	69-70	122	105	109	105	100	127	115	127	127	109	125	98	128	109	119	160	141	206	179	175	169	180	301	196	211	281	235	926	913	940	932	930	933	864	860
6	0445	69-77	107	93	110	97	112	83	113	88	69-77	69-70	69-71	120	100	104	101	92	120	109	117	119	105	118	92	120	104	115	161	136	202	176	162	164	165	301	183	187	292	245	933	928	930	956	924	946	843	842
7	0615	69-74	146	100	151	107	155	77	156	92	69-73	69-70	69-70	145	128	136	132	138	159	142	159	153	131	153	118	148	127	136	200	179	244	213	205	197	198	313	197	220	328	310	950	942	967	969	955	957	880	875
8	0715	69-74	132	95	136	103	139	77	139	87	69-73	69-70	69-70	133	116	123	120	125	145	131	145	143	123	142	111	141	119	129	179	162	228	201	196	189	192	319	187	219	298	277	940	932	966	967	952	958	876	871
9	0830	70-76	115	92	119	101	121	79	120	85	71-75	71	71-72	117	103	107	105	106	129	117	126	129	112	125	100	129	108	120	153	142	211	183	178	175	173	309	184	213	230	224	925	907	945	953	931	945	857	852
10	0945	71-77	174	104	182	108	186	78	185	93	72-75	72-74	73-74	161	145	155	155	164	188	168	183	171	145	167	127	155	131	144	233	214	278	246	225	219	202	332	197	208	374	364	969	966	973	984	965	960	884	877
10A	1030	71-81	211	124	221	127	225	84	226	107	72-79	72-73	72-74	178	166	183	182	212	233	209	229	215	183	209	159	189	163	175	277	257	325	291	273	262	243	365	227	232	402	394	984	981	988	999	973	970	894	886
11	1130	71-75	132	90	135	93	136	77	135	84	71-75	71	70-72	131	117	119	122	117	140	129	134	133	115	130	104	128	108	118	176	168	220	202	181	180	171	289	173	184	298	312	928	937	938	962	942	944	848	842
12	1315	71-77	119	91	118	94	119	83	120	86	71-77	71-72	71-73	121	108	108	110	98	126	115	120	119	104	116	96	117	100	111	153	148	197	182	161	161	160	275	175	170	242	261	898	917	898	941	920	904	802	793
13	1630	68-75	174	120	183	127	180	90	129	108	69-74	69-71	70-72	125	121	140	142	182	199	179	201	190	161	186	152	184	151	168	241	222	305	265	253	243	240	367	232	239	374	358	990	986	996	1005	978	975	897	891
14	1730	69-75	144	104	153	109	151	82	149	95	70-74	70	69-71	106	103	118	120	147	164	150	166	155	133	154	125	154	126	141	211	192	273	233	217	210	208	345	209	219	355	339	982	979	989	999	972	969	892	886
15	1830	69-77	129	100	138	105	136	83	106	92	70-76	70	70-71	99	96	109	110	129	146	133	148	139	119	138	115	141	115	128	198	176	257	214	199	193	194	334	198	211	347	332	978	975	984	995	968	966	889	883
16	2045	68-74	169	114	181	121	176	88	174	103	68-73	68-70	69-71	122	119	136	139	173	194	175	197	182	156	181	142	176	145	162	234	218	297	261	243	238	230	363	224	234	371	354	990	986	995	1005	978	975	896	891
17	2145	68-74	140	101	150	106	148	83	109	92	69-73	69-70	69-70	104	101	115	117	140	160	145	163	151	128	150	119	150	122	136	206	189	268	228	210	205	202	342	202	216	353	337	982	979	988	999	972	970	891	885
18	2300	67-76	222	149	237	158	231	108	158	133	68-75	68-70	68-72	163	159	182	186	238	255	234	259	244	215	239	194	231	196	214	292	272	351	319	307	298	285	405	273	273	412	399	1003	998	1007	1016	989	986	909	902
19	11-17-67 0045	70-73	184	145	199	147	196	108	193	129	70-73	70-71	70-72	126	123	147	148	204	211	194	224	206	180	213	177	200	176	190	258	236	323	281	281	266	267	386	266	260	379	364	996	992	1003	1012	986	983	907	900
20	0130	72-74	161	129	173	133	172	98	171	117	72-74	71-72	71-73	111	109	129	129	178	188	169	195	183	156	185	155	179	153	168	233	209	301	254	254	239	244	370	249	245	355	347	990	986	998	1008	982	980	903	897
21	0230	70-75	228	187	247	191	247	137	247	168	70-75	70-72	71-73	161	157	188	188	266	266	244	277	262	232	266	233	252	224	240	312	283	374	331	342	319	323	424	311	304	412	399	1001	1002	1013	1022	996	993	918	910
22	0315	70-73	214	173	229	174	216	117	213	139	70-73	70-71	70-73	144	142	164	172	222	240	230	254	235	219	244	193	223	203	225	276	265	341	315	300	302	284	411	281	289	392	385	1002	997	1008	1017	991	988	912	904
23	0400	71-73	175	143	186	143	177	99	174	114	70-73	71	71-72	116	115	133	139	179	198	186	206	194	175	197	156	185	163	184	237	223	303	271	256	257	245	380	250	257	357	355	991	987	999	1009	983	980	903	896
24	0515	72-74	170	136	179	140	172	97	171	114	71-74	71-72	71-73	113	112	130	135	177	193	178	196	187	164	186	153	181	154	178	233	217	299	263	252	249	241	375	245	253	355	349	988	984	996	1006	980	977	900	893
25	0615	70-74	204	159	214	165	210	114	212	138	70-74	70-71	70-73	117	134	159	162	222	233	215	237	228	202	225	191	217	188	211	272	252	338	300	298	287	281	400	277	278	386	375	997	992	1004	1013	986	983	906	898
26	0715	70-74	195	153	210	157	199	104	200	132	70-73	70-71	70-72	132	130	151	156	206	222	206	226	217	190	211	176	207	176	201	259	244	325	292	282	277	267	393	266	270	381	370	996	991	1003	1012	986	983	905	898
27	0800	70-75	211	168	228	172	216	114	219	145	70-75	70-71	70-72	145	143	166	172	227	241	226	246	236	211	229	194	225	193	219	279	264	342	311	302	297	285	406	280	284	395	383	1000	995	1006	1015	988	986	909	901
28	1000	71-74	198	150	210	160	201	108	205	133	71-74	71-72	71-73	134	132	154	159	210	228	209	231	222	195	217	178	212	179	203	264	248	329	294	285	280	270	395	267	271	384	371	998	994	1005	1014	987	985	907	900
29	1100	72-74	162	125	173	135	165	93	165	110	72-74	72	72-73	110	109	126	130	167	186	171	189	181	156	177	143	175	147	168	226	210	292	254	241	239	231	369	236	244	353	347	989	985	997	1007	980	978	899	892
30	1315	72-77	174	113	181	119	172	90	127	101	72-76	72-73	72-74	140	132	143	148	169	191	175	192	179	155	174	140	170	144	158	231	219	288	255	236	234	223	354	219	226	377	365	983	980	989	997	973	969	892	884
31	1430	72-78	152	105	159	109	151	87	153	94	73-77	73	73-74	134	122	130	134	145	165	151	166	155	134	151	124	151	128	141	207	195	263	227	211	207	202	337	208	215	359	349	973	968	977	986	961	963	886	880
32	1545	74-81	218	140	229	147	220	106	226	126	74-80	73-75	74-76	167	161	179	183	224	244	224	246	231	201	223	183	217	183	200	281	266	340	306	291	285	269	395	260	259	409	392	998	993	1004	1012	985	980	903	895
33	1745	73-78	166	110	178	114	162	88	119	96	73-77	73-74	73-75	143	134	138	147	152	179	170	188	168	149	170	126	160	140	152	217	213	270	247	216	225	200	344	215	221	369	360	975	971	978	990	966	965	889	882
34	1830	73-78	144	105	156	110	144	86	109	92	73-78	73-74	73-74	138	125	126	133	132	155	149	164	149	133	152	116	149	130	142	193	186	241	219	192	204	184	340	199	216	340	329	956	953	962	979	962	961	884	877
35	1945	74-78	207	131	221	138	204	97	142	111	74-79	74-75	74-76	163	157	167	177	197	227	214	234	214	191	214	160	197	174	190	261	256	317	294	264	274	244	382	233	248	397	388	991	987	996	1006	978	976	895	888
36	2145	76-79	202	137	209	145	182	108	131	131	75-80	75	75-76	136	136	145	161	180	222	205	218	214	180	204	160	203	170	184	240	245	305	285	256	264	248	383	245	251	379	372	989	985	995	1005	977	975	896	890
37	2300	73-77	199	158	216	154	195	117	197	141	73-76	73-74	73-75	139	136	153	161	201	220	209	234	212	190	228	179	207	196	202	257	248	322	294	278	279	267	398	266	269	391	379	1000	995	1006	1015	988	985	908	901
38	11-18-67 0015	74-77	160	129	176	124	161	100	159	115	73-76	73-74	73-74	120	114	127	132	160	174	166	191	168	148	184	144	168	159	162	220	210	284	248	235	233	227	367	234	236	368	357	987	983	994	1005	977	976	896	892
39	0130	73-78	186	155	205	147	198	123	197	144	72-76	72-73	72-74	134	129	151	151	206	209	192	232	204	173	224	187	202	195	191	259	234	324	278	283	263	271	388	267	260	391	371	991	986	997	1006	979	976	900	893
40	0300	74-77	160	128	172	129	166	104	165	123	73-77	73-74	73-74	115	111	129	129	170	183	163	190	178	145	182	153	178	157	161	227	206	294	246	246	230	237	367	239	237	371	351	991	986	998	1007	980	977	901	893
41	0600	71-76	137	99	134	106	134	87	130	100	72-74	72-73	72-73	119	123	114	125	120	143	143	146	142	124	141	113	142	129	136	188	178	233	308	188	197	185	326	184	208	345	326	961	959	969	982	963	961	878	878
42	0650	73-78	165	112	160	120	160	93	155	111	72-75	72-73	72-73	131	135	132	144	152	173	172	177	170	149	169	132	165	143	158	218	209	271	340	220	229	212	361	210	228	372	353	980	975	985	997	974	972	890	888
43	0745	73-84	238	156	245	167	233	120	233	152	73-79	73	73-74	177	177	188	200	235	262	260	264	255	231	257	195	234	206	229	294	289	352	416	307	319	289	422	271	281	422	407	1005	1001	1010	1020	991	989	910	906

3.0 THEORETICAL AND EXPERIMENTAL ANALYSIS

3.1 Background

The original intent of this section was to present the analytical design approaches and performance predictions for the various cask cooling configurations. (Figure 1.2). However, after examining the test results, it became obvious that the functional behavior of the experimental data was not in accord with classical flow theory. Thus at this point there is little to be gained by going through rather involved analytical operations which at best do not give accurate predictions of the problem at hand. Rather these preliminary performance predictions are relegated to a discussion (Section 5.0) of this report and it is more profitable to directly examine the data in light of classical flow theory.

Note that the above comment is not intended to indicate that the classical approach to this design analysis is in error. Instead, as will be subsequently shown, the problem seldom achieves conditions whereby the classical approach may be legitimately applied.

3.2 Basic Open Flow Analysis

In this type of analysis it is conventional to first establish the particular external flow field around the cask, and from this data to determine the local boundary layer characteristics. For heat transfer purposes the boundary layer characteristics would include the effects of both the momentum and energy equations. However at the temperature ranges encountered in this problem, it is adequate and even desirable to simply use the Reynolds analogy to relate the local heat transfer to the local skin friction

For preliminary purposes the external flow may be essentially treated as that emanating from a free jet of suitable geometry. Then the boundary layer skin friction may be obtained through the application of local similarity considerations, i.e., the local external velocity is assumed everywhere constant so that typical uniform velocity solutions may be used (Blasius flat plate, power law distributions, etc.).

The application of these fundamental solutions requires that the problem is well specified. That is, the flow in the jet and/or the boundary layer must be either completely laminar or completely turbulent, the point of flow attachment must be well defined, etc. However when the problem is not well specified it is not entirely reasonable to anticipate reliable predictions from such an approach. For example, the transition Reynolds number for a jet is of the order of 100 as based on the nozzle conditions. When this value is exceeded the flow from a jet will become turbulent, but only after it has traveled a finite distance. Thus the flow must travel the order of 20 nozzle diameters downstream before a fully developed turbulent jet is established. This result is true to a large part, irrespective of the upstream flow conditions. Consequently the initial portion of the external flow on the cylinder as in configuration 1, can not properly be considered either laminar or turbulent. Further since the velocity decay rate is different for a two-dimensional laminar and turbulent jet, it is not clear just what external velocity distribution should be predicted in that region.

A similar problem exists in the boundary layer where again a finite distance is required for a turbulent boundary layer to develop. Also the problem exists that there is a minimum surface Reynolds number to generate and maintain a turbulent boundary layer. Thus even if the outer jet flow is turbulent, it is not necessarily true that the adjoining boundary layer will be turbulent. However in such a situation the corresponding heat transfer in this pseudo laminar boundary layer will be greater than that of an undisturbed laminar boundary layer. Thus from these above comments, as well as others which will be forthcoming, it is apparent that the flow patterns of the various cask cooling configurations seldom achieve a definity of character which would allow a relatively simple type of classical analysis.

Consequently in the almost total absence of any theories for transitional types of flow, it is perhaps more enlightening to look at the evidence, i. e., experimental results, and then trace this information backwards in order to ascertain the particular character of the flow.

For the velocities and temperatures encountered in this experiment, the air may be considered to be an incompressible, perfect gas. If for the moment, the external flow patterns of each cooling configuration are considered to be representative of free jets, then the theoretical velocity decay downstream of the nozzle will be proportional to:

	Laminar	Turbulent
Two-dimensional Jet	$X^{-1/3}$	$X^{-1/2}$
Circular Jet	X^{-1}	X^{-1}

where X is the downstream distance.

Thus for each cooling configuration it might be anticipated that the rate of change of centerline velocity with distance would at least be asymptotic to the proper values in the above table. In Figures 3.1 and 3.2, plots of maximum velocity versus downstream distance are given. Although definite slopes are in evidence in these figures, they are not in agreement with those of the above table. This lack of agreement may be traced largely to two basic sources. First the tabular values are for fully developed flows and these do not occur until the jet, whether laminar or turbulent, has proceeded the order of ten or twenty nozzle diameters downstream - thus it should not necessarily be expected that the initial portion of the flow will follow the classical decay rate. Secondly, the surface of the cask represents a constriction to the otherwise free expansion of the jet - thus the velocity decay rate will be altered by this effect. Also note that the finite transition distance between laminar and turbulent flow will introduce a gradual slope change - at least in the two-dimensional jet.

In all the configurations tested, the nozzle Reynolds numbers exceeded the critical value so that each jet eventually became turbulent. For two-dimensional jets, this transition region is quite easy to locate as in Figures 10 and 11. Upstream of this region the flow has some of the characteristics of a laminar jet, but it is basically undeveloped in terms of classical jet flow. Therefore, it is not to be expected that the laminar jet form would be followed - even if the inherent jet instability has not grown to a significant level to develop into turbulence.

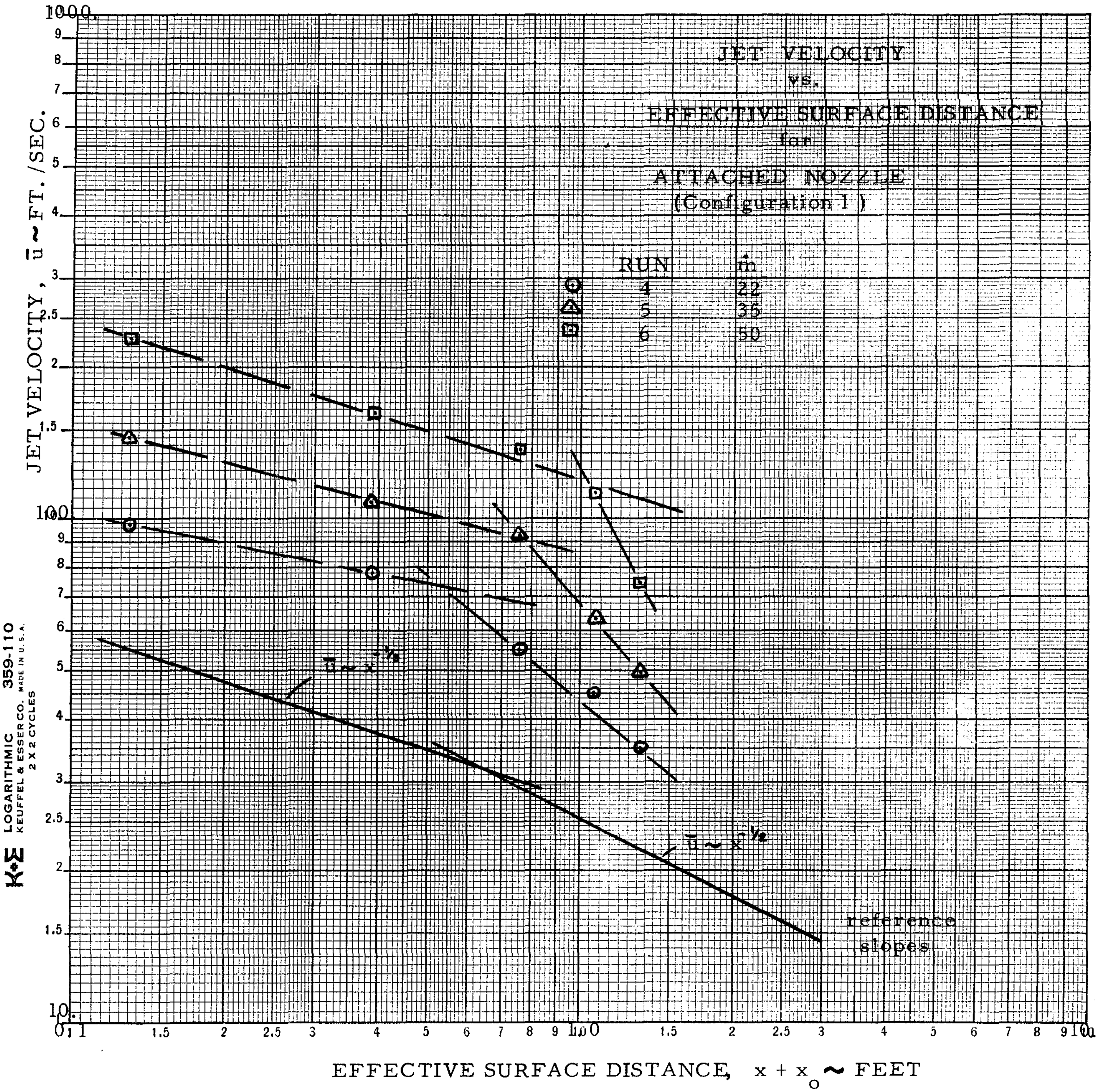
JET VELOCITY
vs.
EFFECTIVE SURFACE DISTANCE
for
ATTACHED NOZZLE
(Configuration 1)
RUN ṁ
4 22
5 35
6 50
JET VELOCITY, ū ~ FT./SEC.
EFFECTIVE SURFACE DISTANCE, x + x_o ~ FEET
ū ~ x^-1/4
ū ~ x^-1/2
reference slopes
LOGARITHMIC 359-110
KEUFFEL & ESSER CO. MADE IN U.S.A.
2 X 2 CYCLES

Figure 3.1

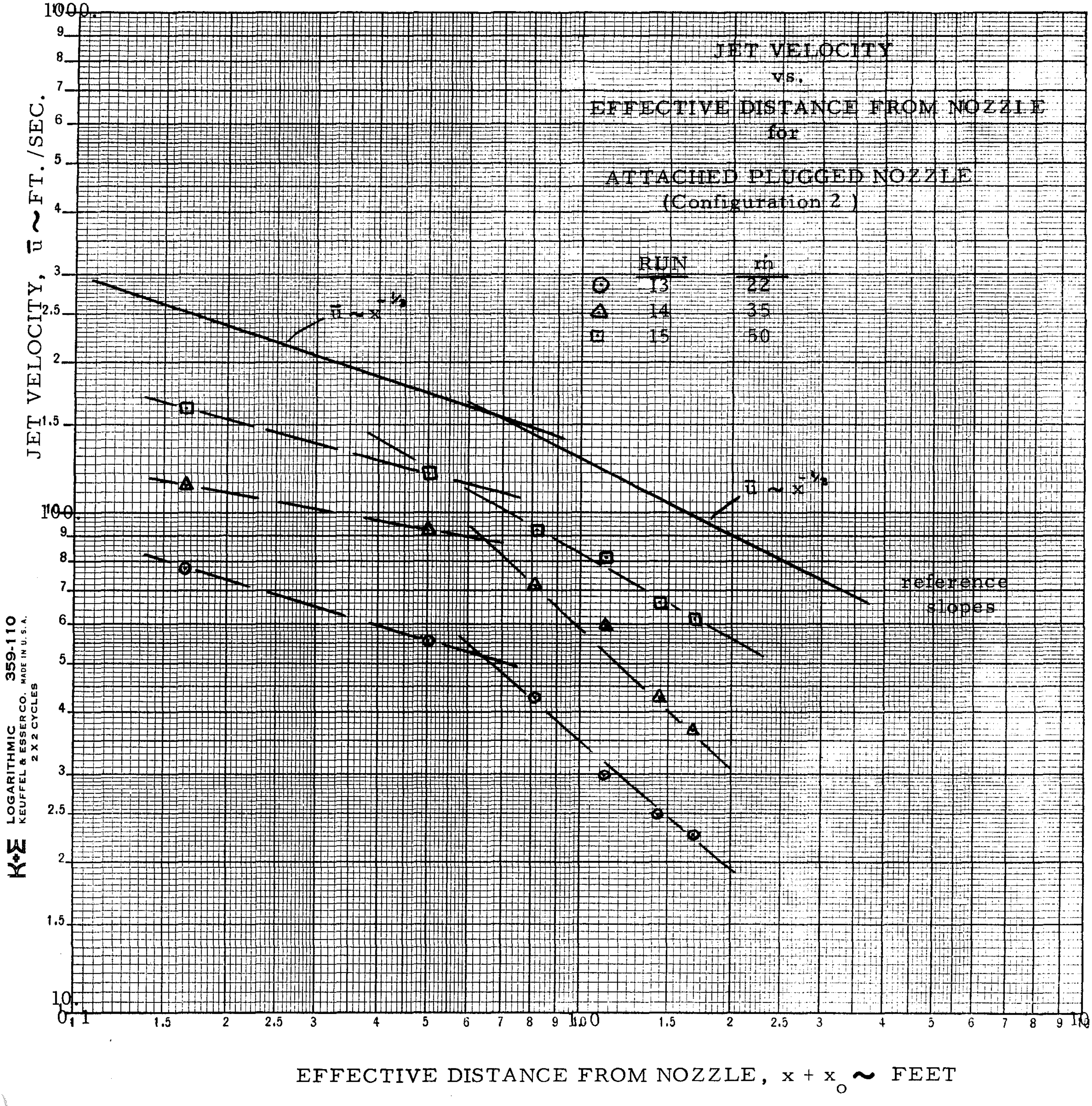
JET VELOCITY
vs.
EFFECTIVE DISTANCE FROM NOZZLE
for
ATTACHED PLUGGED NOZZLE
(Configuration 2)
RUN
ṁ
13
22
14
35
15
50
ū ~ x^-1/3
ū ~ x^-1/2
reference slopes
JET VELOCITY, ū ~ FT./SEC.
EFFECTIVE DISTANCE FROM NOZZLE, x + x₀ ~ FEET
1000.
100.
10.
0.1
1.0
10.
LOGARITHMIC 359-110
KEUFFEL & ESSER CO. MADE IN U.S.A.
2 X 2 CYCLES

Figure 3.2

The net result of the above deviations from theory is that it is easier to look for an empirical data correlation rather than to attempt to reproduce the experimental results with modifications to existing theory. Such an approach is quite justifiable in the case of turbulent jet flows since in the absence of a reliable turbulent transport theory, it is the observed rate of jet spreading which has led to the accepted velocity decay rates. On the other hand, at least until flow impingement on the cask, the circular jet will behave as theoretically predicted since the laminar and turbulent velocity decay rates are the same.

Assuming that the external flow velocities are now available, it is next necessary to establish the boundary layer characteristics and thereby the shear and heat transfer at the cask surface. For a perfect, incompressible gas, the Reynolds analogy may be written

$$St = \frac{1}{P_r^{2/3}} \quad C_{f/2}$$

Therefore the film coefficient, h, will be

$$h = \frac{Q}{A \Delta T} = \frac{St \rho \, g u C_p \Delta T A}{A \Delta T}$$

or

$$h = \frac{\rho \, g \, u \, C_p}{P_r^{2/3}} \quad C_{f/2}$$

By considering each segment of the cask to be essentially a flat plate, the skin friction may be related to a local Reynolds number. However the main difficulty is in establishing a reference distance upon which to base this local Reynolds number. For configuration 1 this orientation is no problem, but for the detached nozzles, the effective initial point of flow contact is not obvious. In order to temporarily bypass this problem it is possible to make direct use of the experimental data and thereby determine the sensitivity of the film coefficient to the effective point of flow attachment.

For laminar flow on a flat plate the skin friction is proportional to $R_{e_x}^{-1/2}$ and for fully developed turbulent flow on a flat plate the skin friction is approximately proportional to $R_{e_x}^{-1/5}$. For each location on the cask at each flow configuration, the effective surface distance is approximately constant so that

$$C_{f/2})_{Lam} \sim u^{-1/2}$$

$$C_{f/2})_{Turb} \sim u^{-1/5}$$

In addition at each location on the cask the source heat per unit area (Q/A) is essentially fixed. Thus the film coefficient will be inversely proportional to the difference between the wall temperature and the free stream temperature, i. e.,

$$h \sim \frac{1}{T}$$

Consequently for each station and configuration we may write

$$\sqrt{u}\,\Delta T = \text{const.} \qquad \text{(laminar flow)}$$

$$u^{0.8}\,\Delta T = \text{const.} \qquad \text{(turbulent flow)}$$

Upon plotting the experimental values of u and ΔT for various thermocouple locations on the cask, it is somewhat surprising to find that on log-log paper the entire set of primary test data can nearly be correlated with one straight line (Figures 3. 3, 3. 4, 3. 5). (Note that the term primary is here applied to the non-interferred portion of the cask surface, i. e., the front side. This is the only portion of the data where some direct correlation can be anticipated a priori.) However the slope of this experimental curve follows neither the laminar nor the turbulent value.

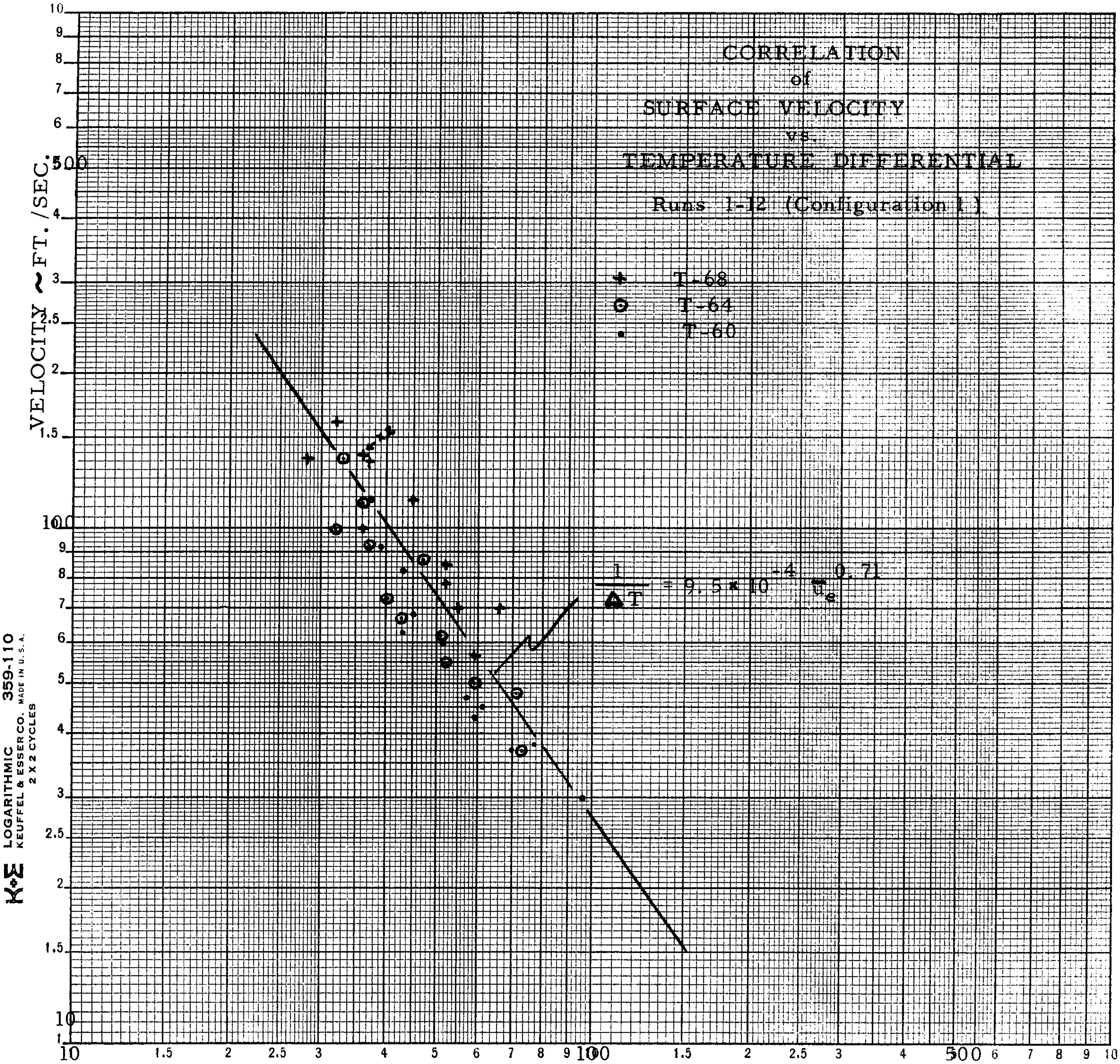
CORRELATION
of
SURFACE VELOCITY
vs.
TEMPERATURE DIFFERENTIAL
Runs 1-12 (Configuration 1)
T-68
T-64
T-60
$\frac{1}{\Delta T} = 9.5 \times 10^{-4}\ \bar{u}_e^{0.71}$
VELOCITY ~ FT./SEC.
TEMPERATURE DIFFERENTIAL, ΔT ~°F
359-110
LOGARITHMIC
KEUFFEL & ESSER CO. MADE IN U.S.A.
2 X 2 CYCLES

Figure 3. 3

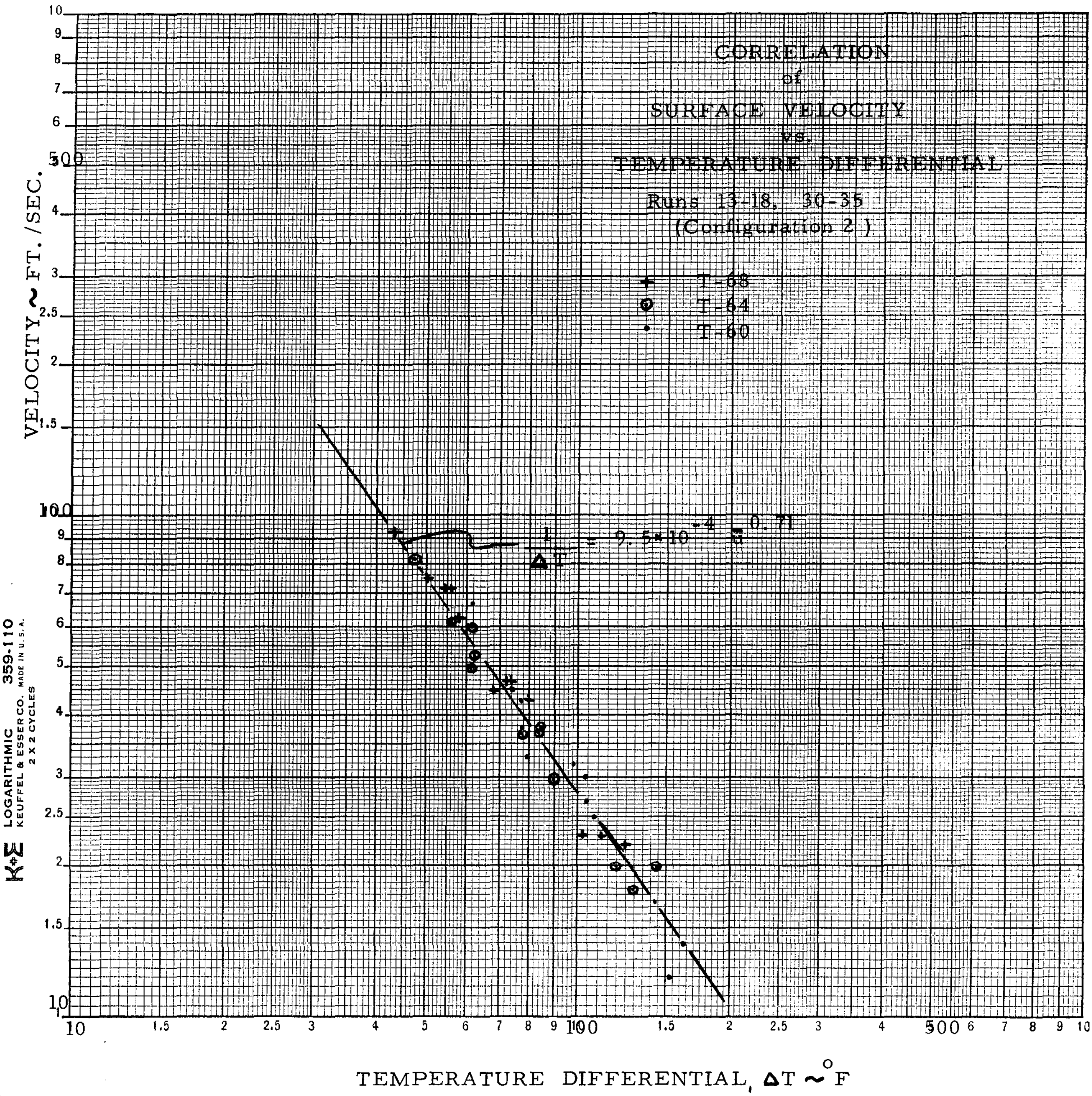
CORRELATION
of
SURFACE VELOCITY
vs.
TEMPERATURE DIFFERENTIAL
Runs 13-18, 30-35
(Configuration 2)
T-68
T-64
T-60
= 9.5*10-4
0.71
VELOCITY ~ FT./SEC.
TEMPERATURE DIFFERENTIAL, ΔT ~ °F
LOGARITHMIC 359-110
KEUFFEL & ESSER CO. MADE IN U.S.A.
2 X 2 CYCLES

Figure 3.4

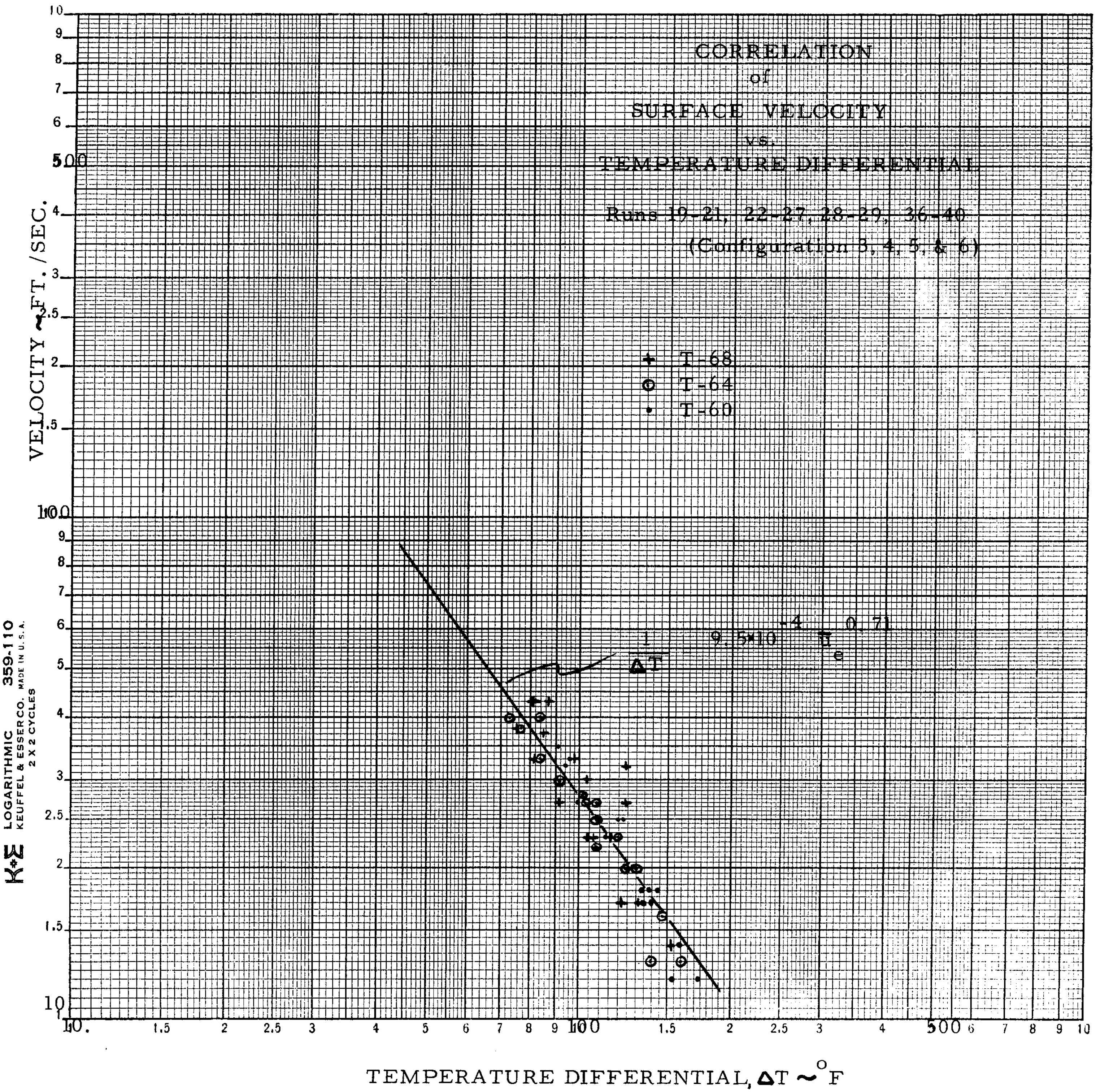
CORRELATION
of
SURFACE VELOCITY
vs.
TEMPERATURE DIFFERENTIAL
Runs 19-21, 22-27, 28-29, 36-40
(Configuration 3, 4, 5, & 6)
T-68
T-64
T-60
$\frac{1}{\Delta T} = 9.5 \times 10^{-4} \, \overline{u}_e^{\,0.71}$
VELOCITY ~ FT./SEC.
TEMPERATURE DIFFERENTIAL, ΔT ~ °F
10
100
500
K+E LOGARITHMIC 359-110
KEUFFEL & ESSER CO. MADE IN U.S.A.
2 X 2 CYCLES

Figure 3.5

Irrespective of the slope of surface velocity versus ΔT, some streamwise variation in the proportionality between the velocity and temperature increment might be anticipated. However only in the case of the attached nozzle (configuration #1) is any such dependence evident. This particular case most nearly approximates the boundary layer flow along a flat plate (with an adverse pressure gradient) where a flow initiation point was well defined.

Since the streamwise boundary layer dependence decreases with increasing streamwise distance, the detached nozzle flows, which all the others are, have evidently become attached far enough upstream in relation to the placement of the three surface thermocouples on the cask cylinder (T-68, T-64, and T-60) to effectively reduce the streamwise boundary layer dependence to a negligible level. This is not to say that the boundary layer characteristics are not changing as the flow proceeds downstream, but that the cumulative effects of an external velocity decay and a lag in the adjustment to local similarity in the cask cylinder have resulted in a shear coefficient (or Stanton number) which is essentially independent of streamwise distance. Such behavior is in contrast to the classical skin friction dependence noted above where a constant external velocity is assumed throughout to develop such theories.

Note that none of the above comments include the fully shrouded case (configuration 7) which requires a separate form of analysis.

Since a correlation now exists between the velocity and the temperature differential on the open side of the cask, it is possible to combine this correlation with the previously established correlation of velocity and upstream flow conditions parameters to yield a relation between the air supply parameters and the surface temperature rise. In addition it is somewhat fortuitous that the maximum measured surface temperature, which occurs at T-61, is always within several degrees of being 10% higher than the temperature at T-60, which is one of the correlated values. Thus a correlation between the air supply conditions and the maximum surface temperature is relatively easy to establish. For the attached nozzle (configuration 1) there should be some streamwise dependence of ΔT other than what is obtained from the basic external velocity decay. However the data scatter exceeds whatever variation might be predicted so that in the interest of overall simplicity, it is accepted that all the experimental data of configurations 1 through 6 essentially obeys the relation:

$$\frac{1}{\Delta T} = 9.5 \times 10^{-4} \quad u_e^{0.71}$$

Note that this slope (0.71) lies between the aforementioned laminar and turbulent values (0.5 and 0.8).

Although all the attached and plugged nozzles (configurations 1, 2, and 4) essentially generate two-dimensional jets at the onset of the flow, only when the nozzle is relatively close to the cask is the basic characteristic of this flow preserved. That is, as these nozzles are placed further from the cask, the expanding two-dimensional jets eventually merge because of their circular placement. Thus their velocity decay (which is directly related to the jet expansion area through the momentum equation) changes its form as the flow loses its two-dimensional characteristics.

Consequently it is not possible to conveniently apply a single velocity decay formula to the plugged nozzle. Initially an attempt was made to find a modified velocity decay versus downstream distance through logarithmic plots. However this slope is also a function of the ficticious source point in the nozzle. After a considerable amount of data manipulation, it appeared that the best compromise would be to use the basic axisymmetric form, but with a different value of the empirical constant which necessarily appears in all turbulent flow formulations (Figures 3.6, 3.7). This formulation is reasonably adequate for the attached nozzle as well, so that all the velocity distributions may be expressed in basically the same form.

Note that in the above commentary no mention is made of the velocity distribution across the jet. However in essentially all the cases, the maximum velocity occurred in close enough proximity to the cask wall so that the centerline velocity effectively approximates the edge velocity of the boundary layer along the cask wall. Also no consideration is given to the blockage of the flow by the cask itself. Because of the relative size of the cask and jet dimensions, it might be expected that this effect would be significant. However the fact that the experimental correlation is adequate is justification enough for neglecting the presence of the cask in calculating the streamwise velocity distribution.

Consequently the inviscid flow adjacent to the cask and emanating from an axially aligned two-dimensional jet may be written

$$u_e = \frac{54 \sqrt{\dot{m}} \quad \Delta p^{1/4}}{x + 1.9 \quad \sqrt{\dot{m}/\Delta p^{1/4}}}$$

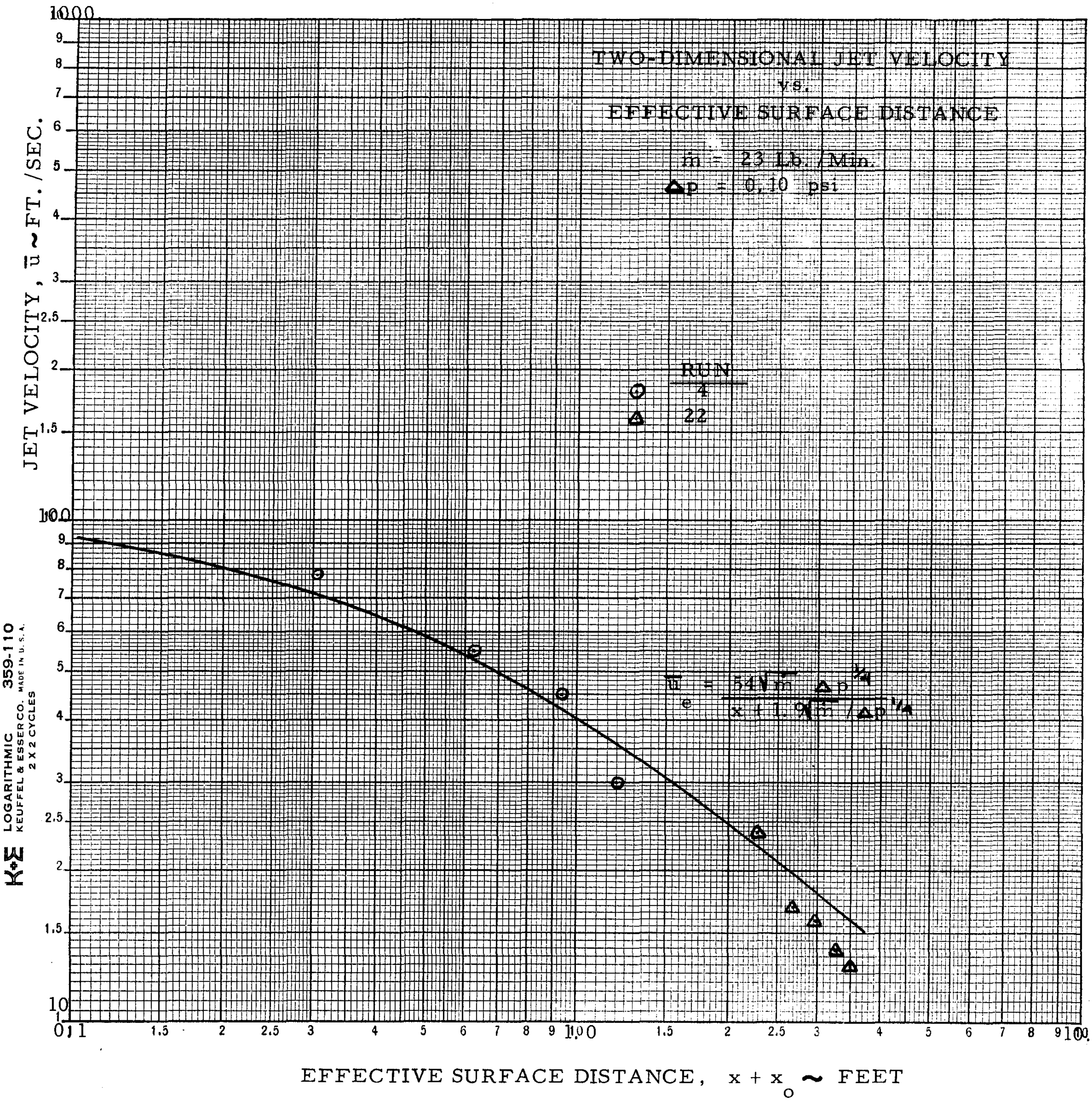
TWO-DIMENSIONAL JET VELOCITY
vs.
EFFECTIVE SURFACE DISTANCE
ṁ = 23 Lb./Min.
Δp = 0.10 psi
RUN
4
22
$\bar{u}_e = \dfrac{54\sqrt{\dot{m}}\ \Delta p^{1/4}}{x + 1.9\sqrt{\dot{m}}/\Delta p^{1/4}}$
JET VELOCITY, ū ~ FT./SEC.
EFFECTIVE SURFACE DISTANCE, x + x$_o$ ~ FEET
LOGARITHMIC 359-110
KEUFFEL & ESSER CO. MADE IN U.S.A.
2 X 2 CYCLES

Figure 3.6

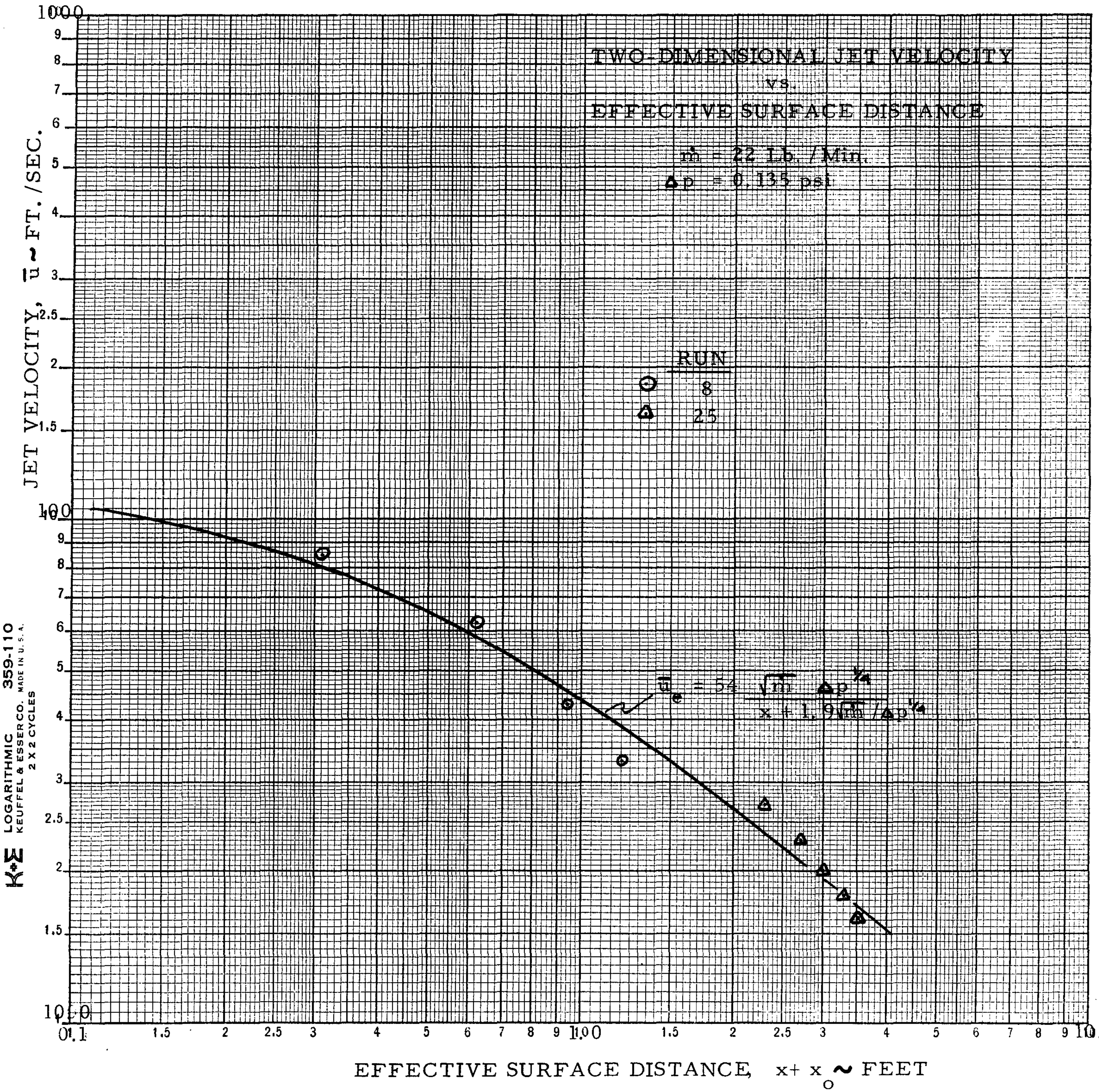
TWO-DIMENSIONAL JET VELOCITY
vs.
EFFECTIVE SURFACE DISTANCE
$\dot{m}$ = 22 Lb. /Min.
Δp = 0.135 psi
RUN
8
25
$\bar{u}_e = 54 \frac{\sqrt{\dot{m}}\ \Delta p^{1/4}}{x + 1.9\sqrt{\dot{m}}/\Delta p^{1/4}}$
JET VELOCITY, $\bar{u}$ ~ FT. /SEC.
EFFECTIVE SURFACE DISTANCE, $x + x_o$ ~ FEET
LOGARITHMIC 359-110
KEUFFEL & ESSER CO. MADE IN U.S.A.
2 X 2 CYCLES

Figure 3.7

where from the basic form

$$u_{\mathbb{C}} = \frac{3}{8\pi} \quad \frac{K}{\epsilon\,(x + x_o)} \quad , \quad K = \int u_{ex}^2 \, dA$$

$\epsilon = 0.043 \sqrt{K}$ instead of $0.016 \sqrt{K}$ as in the classical circular jet. Upon combining this result with the above temperature - velocity correlation, the temperature differential becomes

$$T = 62 \left[\frac{x + 1.9 \quad \sqrt{\dot{m}/} \quad p^{1/4}}{\sqrt{\dot{m}} \quad p^{1/4}} \right]^{0.71}$$

where

$\dot{m}$ = mass flow $\sim$ lb/sec

$\triangle p$ = pressure differential $\sim$ psf

x = distance from the nozzle to a point on the cask cylinder $\sim$ ft.

This equation is plotted in Figures 2.2, 2.3, and 2.4 for a realistic range of the involved parameters. Note that this temperature differential represents that of the open side of the cask. Therefore the maximum cask wall temperature will be approximately 10% higher than the absolute value of the wall temperature at maximum x of the cask cylinder. Also note that the apparent wide discrepancy between this correlation and several of the experimental runs is largely a result of the partial misalignment of the plugged nozzle relative to the cask. Thus especially at the lower mass flows and pressures, nozzle alignment is an important factor.

For the circular jets, (configurations 3, 4, and 6) a similar approach gives a velocity distribution as:

$$u_e = \frac{77 \cos \theta \, \Delta p^{1/4} \sqrt{\dot{m}}}{x + \dfrac{2.7 \sqrt{\dot{m}}}{\Delta p^{1/4}}}$$

where in this situation, θ is the angle between the jet axis and the cask axis ($0 \leq \theta \leq 45^{\circ}$). Except for the angular correlation, this form is in agreement with the classical laminar and/or turbulent distribution. Upon combining this form with the temperature - velocity correlation, the cask temperature differential for circular jet cooling on the front side of the cask becomes (Figures 2.5, 2.6, and 2.7)

$$\Delta T = 48 \left[\frac{x + \dfrac{2.7 \sqrt{\dot{m}}}{\Delta p^{1/4}}}{\cos \theta \, \Delta p^{1/4} \sqrt{\dot{m}}} \right]^{0.71}$$

where

$\dot{m}$ = mass flow $\sim$ #/sec

Δp = pressure differential $\sim$ psf

θ = angle between nozzle axis and cask axis ($0 \leq \theta \leq 45^{\circ}$)

x = actual distance between nozzle and front side cask surface point.

Again the maximum cask surface temperatures occur on the sides of the cask and are approximately 10% higher than the absolute temperatures of the open side. Note that it is precisely the presence of the radiation heat shield which directs the flow up the back side of the cask when the nozzle is off center with respect to the cask axis. Under this situation the back side temperatures are at least as low as the front temperatures. However removal of the radiation shield would completely disrupt this back side cooling.

3.3 Correlation of Open Flow to Theory

From the standpoint of future analysis as well as academic interest, it is useful to compare the effective skin friction coefficient as obtained through the above data correlation with that of the skin friction predicted through classical boundary layer theory. Since the above correlation essentially bypassed the need for film coefficients and internal thermal analysis, no effective surface area was established. However for purposes of comparison, a projected geometric area and a uniform internal heat source should provide adequate estimates of the actual values. As noted above, by the Reynolds analogy, the skin friction coefficient may be written as:

$$C_{f/2} = \frac{P_r^{2/3} \quad h}{\rho g u C_p} = \frac{P_r^{2/3} \quad Q}{\rho g u C_p \triangle T A}$$

Also by the cask wall data correlation

$$\frac{1}{\triangle T} = 9.5 \times 10^{-4} u_e^{0.71}$$

Combining these equations yields

$$C_{f/2} = \frac{9.5 \times 10^{-4} \quad P_r^{2/3} \quad Q}{\rho \; g \; C_p \, A \, u^{0.29}}$$

The net heat output is 1500 watts or 1.4 BTU/sec and the effective area of this cask is of the order of

$$A \simeq \pi \times \frac{8}{12} \times \frac{20}{12} = 3.5 \text{ sq. ft.}$$

Using these values of Q and A plus an air Prandtl number of 0.71, the skin friction coefficient becomes

$$C_{f/2} = \frac{0.0165}{u_e^{0.29}}$$

Because of a lack of dependence upon streamwise distance in the data correlation for ΔT, it is necessary to assume some effective surface distance if the above skin friction coefficient is to be compared to the classical values which are functions of Reynolds number, i.e.,

$$C_{f/2} = C_{f/2}(R_{e_x}) = C_{f/2}\left(\frac{\rho u_e X}{\mu}\right)$$

Since the exponent of u_e is 0.29, the Reynolds number and thus X will be raised to this power. In reality X varies from approximately 0.5 to 3.0, but upon raising this to the 0.29 power, this is only a variation from 0.8 to 1.3 or a factor of $\pm$30%. This variation at least allows a rough comparison with the classical values of $C_{f/2}$. Using a nominal value of 1.5 for X, the experimental skin friction coefficient becomes

$$C_{f/2} = \frac{0.23}{(R_{e_x})^{0.29}}$$

In the table below this form compared with the accepted flat plate turbulent values. (Note that the Stanton number $\simeq$ 1.25 $C_{f/2}$).

R_{e_x}	$C_{f/2} \times 10^3)_{Exp.}$	$C_{f/2} \times 10^3)_{F.P.}$
10^5	8.1	3.8 (2.1 Lam.)
10^6	4.2	2.3
10^7	2.1	1.4

As can be seen, the projected experimental values of $C_{f/2}$ exceed the pure flat plate values by more than the uncertainty in X. Further if some X variation with Reynolds number had been allowed in these projected values of $C_{f/2}$, then the disparity would be greater. Although the cask surface is quite rough, subsequent calculations indicated that this condition would at most result in a small increase in the skin friction at the lower Reynolds number. Therefore the observed skin friction increases are probably attributable to the high level of free stream turbulence and the lag in boundary level development.

With respect to the lag in boundary layer development, there are two contrasting factors which result in a seemingly anomalous behavior of the boundary layer. However upon looking more closely at the boundary layer structure, the results are seen to be plausible and even expected. For a typical laminar boundary layer on a flat plate, there is a certain similarity at the various streamwise locations. That is, the individual boundary layer profiles may all be reduced to the same profile by an appropriate choice of scale factors. However when there is turbulence in the free stream, the momentum transfer to the external portion of the laminar boundary layer from the free stream is considerably increased. Therefore the effective laminar boundary layer is much thinner, than as predicted by the similarity solutions - which results in a higher velocity gradient near the wall and thus a much higher value of skin friction. Such a situation exists in the region of flow attachment on the cask where the Reynolds number is initially low and even after reaching the transition level, there is a finite distance required to achieve transition. A similar situation, though to a lesser extent, exists with the turbulent boundary layers. That is, the free stream turbulence has somewhat of a thinning effect upon even a turbulent boundary layer where ordinarily the turbulence level decreases in the outer portions of the boundary layer. Thus the distribution and magnitude of the disagreement between classical and present experimental skin friction coefficients is relatively easily explained by the fact that all the jet flows tested were themselves turbulent - thereby resulting in a high level of free stream turbulence.

However there still exists the problem of the lack of streamwise dependence of the skin friction. At first glance this independence might appear to be the result of an excessive lag in the boundary layer development so that the streamwise position has little effect upon the wall shear. The alternative to this viewpoint is that the high level of turbulence throughout the boundary layer results in a very rapid adjustment of the boundary layer. Thus the boundary layer behaves similarly to the fully developed flow between parallel walls, where the distance between the walls is the characteristic distance. Owing to the high level of turbulence in the outer flow (and the resultant increased wall shear) it appears that the second viewpoint is the valid one. Therefore the lack of streamwise shear dependence would indicate that there are compensating effects which result in an almost negligible change in the effective boundary layer thickness - or more properly, the momentum thickness of the boundary layer is essentially independent of the streamwise position. These compensating effects are probably located in the rate of growth of the turbulent intensity, both within and without of the boundary layer. That is, especially in the situation where the nozzle and cask are relatively close and thus a greater streamwise variation would be expected, the normal time (or streamwise) delay in the development of the turbulent intensity in both the free stream and the boundary layer results in increasing transport across the boundary layer as the flow proceeds downstream - thereby resulting in a negligible change in the boundary layer momentum thickness and thus a negligible change in wall shear as a function of position, i. e.,

$$\frac{\tau}{\rho u^2} = \frac{d\theta}{dx} + \delta^* u \frac{du}{dx} .$$

Note however that there is a wall shear drop resulting from the streamwise decay of the external velocity.

3.4 Shroud Analysis

The experimental values of the heat transfer for the shrouded case also exceed the theoretical predictions by a considerable amount. The theoretical analysis, as presented in the appendix, was based on a smooth walled, fully developed channel flow. Since the geometry of the shroud rather faithfully represents a channel flow system, the differences in the heat transfer between theory and experiment must be represented by the conditions imposed upon the two-dimensional flow, i. e., the smooth wall, the fully developed flow, and possibly the form of the Reynolds analogy.

While the degree of roughness of the cask wall was not significant in increasing the shear of the relatively thick open flow boundary layers, the same roughness can be significant in a shrouded system where the boundary layer growth is constrained. Although the surface roughness of the test cask was far from uniform, the average roughness appears to be of the order of one mil. Thus the ratio of the channel height to the roughness height is of the order of 200. For the Reynolds numbers of the shroud experiments (3,000 - 10,000), it does not appear that such a roughness ratio would contribute more than a 10% increase to the wall shear. However these estimates are based upon pipe flow results since there is very little experimental data for roughness in two-dimensional flow. Therefore because the flow conditions are in a region of high sensitivity to roughness, it is possible that the projected value of a 10% increase in wall shear could be either markedly high or low. Also note that some of the rougher local areas on the cask wall would result in a higher local shear.

In well controlled experiments, it is usually necessary for a flow to travel at least 50 inlet dimensions downstream before fully developed channel flow is achieved, (either laminar or turbulent). Up to that point the wall velocity gradients are much higher because the center portion of the flow has not yet adjusted to the wall shear effects. Consequently it is to be expected that the experimental film coefficients would exceed the predicted values over at least the majority of the cask cylinder. The Reynolds numbers for the three test runs were all sufficiently large to maintain turbulent channel flow so it appears that the shroud flow is going in that direction. In the table below, the Reynolds numbers, the predicted film coefficients, and the measured film coefficients are given for the three shrouded flow tests.

Run	R_e	h_{calc} (BTU/Hr ^oF ft^2)	h_{T-68}	h_{T-64}	h_{T-60}
41	10,800	16.	29.	26.	20.
42	7,400	12.	21.	18.	14.
43	3,200	6.6	11.	9.	7.6

Note that the decrease in the measured values of h as the flow proceeds downstream is not entirely a result of the gradual development of the channel flow. There is also the factor of $(1 - T_e/T_w)$ which represents the decrease in heat transfer resulting from the increase in air temperature. As may be seen in the preliminary shroud design in the appendix, this factor can represent a significant reduction in heat transfer - especially in the case of low mass flows and thus low total heat capacity of the cooling air.

Since there is little valid data and no complete theory for turbulent flow, it is not possible to apportion the relative importance of the factors which effectively increased the film coefficients in the shrouded flow tests. While it might appear that a lag in the development of the channel flow was the major contributor (as opposed to the surface roughness), the accuracy of the applied form of the Reynolds analogy in such a flow is certainly subject to question.

However in light of the success of the open flow cooling systems, there does not appear to be any point in attempting to generate a valid and plausible means to predict the actual heat transfer which is attained from the more cumbersome shroud system.

4.0 THERMAL CORRELATION

Although a thermal analysis was not used (or necessary) in the correlation of the experimental data, several analyses were carried out to verify that the experimentally derived film coefficients were compatible with the measured cask temperatures. The basic model for the thermal analysis employs a finite difference approach wherein the physical configuration is subdivided into discrete finite elements - each of which is assumed to be isothermal. The mass of each element is assumed to be concentrated at its geometric center and is termed a node. These nodes have arbitrary individual heat sources and are linked together in a resistance network analogous to that of an electrical circuit. In this analogy the temperature is the analogue of the voltage and the heat flow is the analogue of the current.

For purposes of comparison, test runs 4, 5, and 6 were numerically analyzed using the graphite material properties as supplied by G. E. for the Super Temp Cask. A 26 node model was used for this analysis and in Table IV the predicted and measured temperatures are given for these nodes - along with the film coefficients as supplied from the test analysis of Section 3.4. Since no cask liner was used in these tests, the internal air essentially acted as an oven to moderate the temperatures between the capsule and the cask, as well as along the cask. Thus the various temperature gradients were not excessive, and thereby the nodal cask temperatures could be legitimately averaged in the analyses.

While the correlation between the predicted and averaged, measured temperatures is not exceptionally good, it is close enough within the bounds of the method of analysis. Further refinement of the model and the internodal properties could undoubtedly bring the predicted temperatures closer to the individual measured temperatures. However this upgrading would be a somewhat of a post factum approach. Rather the basic point to be made is that the film coefficients as developed in Section 3.4 are in the proper range for the measured temperatures.

TABLE IV

CASK TEMPERATURE CORRELATIONS

FILM COEFFICIENT, h ~ BTU/HR, FT^2 ^oF

TEMPERATURES ~ ^oF, PREDICTED & MEASURED

Location	Free Conv.		Test Run #4		Test Run #5		Test Run #6	
	h	Pred/Meas	h	Pred/Meas	h	Pred/Meas	h	Pred/Meas
Barrel (SLA)	1.0	527/529	24.0	133/137	34.0	115/119	45.0	105/113
Barrel (Shield)	1.0	556/556	25.0	132/130	34.0	116/108	48.0	103/104
Band (upper)	1.0	430/463	5.8	127/140	9.2	108/114	13.1	96/112
Band (lower)	1.0	432/457	26.9	97/94	38.5	87/89	46.0	82/90
Dome (upper)	1.5	364/377	6.8	121/129	11.0	103/110	15.4	93/106
Dome (lower)	1.0	437/	3.9	169/	4.8	155/	6.1	142/
Shield (front)	1.5	117/105	25.0	70/70	34.0	70/70	39.3	70/70
Shield (rear)	1.0	75/	1.0	70/	1.0	70/	1.0	70/
Barrel In. (SLA)	0.3	560/571	0.3	183/195	0.4	166/175	0.4	155/168
Barrel In. (Sh)	0.3	586/589	0.3	182/196	0.4	166/176	0.4	154/175
Fuel		1419/-		1313/-		1311/-		1310/-
Capsule	0.4	1017/1001	1.0	899/873	0.9	896/862	0.9	895/842
End Plate	0.7	570/581	1.0	328/312	1.0	317/258	1.0	311/269
Internal Air		634/-		225/-		221/-		218/-
LM	1.0	77/85	1.0	70/70	1.0	70/70	1.0	70/70
SLA	Sink	70/70	Sink	70/70	Sink	70/70	Sink	70/70

5.0 DISCUSSION OF PRE-TEST ANALYTICAL STUDIES

5.1 Axial Flow Air Cooling Systems

5.1.1 Attached Nozzle - Open Flow

In a highly convergent nozzle such as this, (Drawing 2) the volocity at the nozzle exit is essentially uniform in distribution and equal to the Bernoulli value times some discharge coefficient

$$(U_{ex} = \sqrt{\frac{2 \triangle p}{\rho}} \; C_D).$$

It is then necessary to establish the subsequent velocity decay as the flow proceeds along the cylinder. For the present purposes of analysis, it was assumed that the velocity decay of a corresponding two-dimensional free jet would yield an adequate initial estimate. Such an approximation is justifiable because of the counteracting effects of the presence of the wall - one of which restricts the flow expansion and thereby tends to retard the rate of velocity decay, while the other, the wall friction, tends to increase the rate of velocity decay.

The basic problem lies in the determination of the character of the boundary layer flow, i.e., laminar or turbulent. The critical Reynolds number for a two-dimensional nozzle is of the order of 50 as based on the height of the nozzle. For the application under consideration here, the Reynolds number is at least an order of magnitude greater than 50. Therefore the flow issuing from the nozzle will become turbulent. However this does not necessarily mean that the boundary layer flow along the wall will be turbulent. Downstream of the nozzle, the nozzle turbulence may be regarded as free stream turbulence - and while this free stream turbulence will tend to promote the transition to turbulence in the boundary layer, unless the wall Reynolds number is sufficiently high to support turbulence, there will be no transition to turbulent flow at the wall.

Consequently the basic flow pattern on the cask wall is initially laminar with a high level of free stream turbulence. Then as the Reynolds number increases along the cask (which it does - although somewhat diminished by the jet velocity decay) the flow would enter a transition phase and eventually become fully turbulent. However in the relatively short length of the cask wall, it is not clear that the flow would ever achieve a fully developed turbulent boundary layer, and in some cases, transition itself may not be attained.

As the basic jet will be turbulent in all cases, the centerline velocity decay rate may be taken as that of the turbulent value for a two-dimensional jet. In order to calculate the heat transfer, a local similarity may be assumed with the free stream velocity equal to that of the local mean jet velocity.

It is then necessary to make some estimate of the character of the boundary layer flow at each point along the wall. Because of the presence of free stream turbulence in the main flow, the heat transfer in the laminar portion of the boundary layer will be greater than that of purely laminar flow. Then as the flow proceeds downstream and through transition, the turbulent heat transfer value will probably be approached - although it is doubtful that the actual value will be attained in such a short distance.

Since no methods exist for predicting heat transfer in transitional flow, only qualitative estimates of the heat transfer may be made where this type of flow occurs. However if the level of free stream turbulence may be estimated, then it is possible to predict the increase in heat transfer in the laminar flow regime. This value will then furnish a lower bound for the local heat transfer. Beyond that point it is purely a matter of estimation as to what level of turbulence and its corresponding heat transfer are attained as the flow proceeds downstream. In the extreme cases, the flat plate Reynolds number will furnish a criterion for the location of the transition region and fully developed turbulent flow, but in the intermediate cases, no such criteria exist. Thus a wide tolerance in the predicted heat transfer will be necessary until actual experimental data becomes available.

As a typical design example, the following case is developed.

The available pressure differential at the nozzle is taken to be 1 psi. Thus the mean exit velocity (corrected by a discharge coefficient of 0.8 would be:

$$\bar{u}_{ex} = 0.8 \sqrt{\frac{2 \times 144 \times 1}{0.002378}} = 278 \text{ fps}$$

For a mass flow of 50 #/min, the height of the nozzle would be

$$H = \frac{\dot{m}}{\rho g\, u_{ex}\, b} = 0.019 \text{ ft.}$$

Therefore the nozzle Reynolds number would be

$$R_e = \frac{278 \times 0.019}{1.65 \times 10^4} = 3.2 \times 10^4$$

which is well above the critical value for a two-dimensional jet, i.e., the basic jet will be turbulent.

The centerline velocity decay of a two-dimensional turbulent jet may be written as:

$$U_{\mathfrak{L}} = \frac{\sqrt{3}}{2} \sqrt{\frac{K\sigma}{x + x_o}}$$

where

$$K = \int U^2 dy = U_{ex}^2 \ell$$

$$\sigma = 7.7 \text{ (experimental value)}$$

x_o = fictitious reference point to match $U_{\mathfrak{L}}$ with U_{ex}

For the free stream velocity along the wall, the average of the jet velocity is used, which is approximately 2/3 of the centerline velocity. With the above information, the free stream velocity and the corresponding local Reynolds number may be calculated as a function of the distance along the cask. In the table below, these values are given for the initial conditions

$\dot{m}$ = 50 #/min

p = 1 psi

C_D = 0.8 (discharge coef.)

X(in)	$X+X_o$(ft)	U_e(fps)	$R_{e_x} \times 10^{-4}$	h(BTU/Hr ft^2 ^oR)
0	0.11	180	1.2	9.5 - 24
2	0.28	113	1.9	6.0 - 15
4	0.44	91	2.4	4.8 - 12
6	0.61	77	2.8	4.1 - 10
8	0.78	68	3.2	3.6 - 9
10	0.94	62	3.7	3.3 - 8.3
12	1.11	57	3.8	3.0 - 7.5
14	1.28	53	4.1	2.8 - 7

The film coefficient values (h) given at the right of this table represent the upper and lower bounds which might be anticipated. These values were obtained from Volume 5 of the Princeton Series, "Turbulent Flows and Heat Transfer". In order to reduce the spread in the film coefficient as given above, it will be necessary to conduct experimental testing under the properly simulated conditions.

5.1.2 Detached Nozzle - Open Flow (Drawing 3)

Although the flow pattern for this type of nozzle is somewhat different from that at the attached nozzle, the approximations inherent in any turbulent flow analysis render the two problems virtually identical in terms of the applied numerical analysis. Thus except for a relocation of the streamwise coordinate (X), the preceding analysis (extended in X) will suffice for the preliminary heat transfer estimates.

5.1.3 Attached Nozzle - Shrouded Flow (Drawing 4)

The basic purpose of the cylindrical shroud is to constrain the expansion of the axial flow so that there is no velocity decay or flow separation. The flow pattern is essentially that of two-dimensional flow between parallel plates. However although the Reynolds numbers are adequate to maintain turbulent flow, it is not evident that fully developed flow would be achieved in such a short distance. This lag is partially a result of the inlet affects and partially a result of the finite time (distance) required for flow transition.

Two approaches are available to analyze this system. One approach is to use only gross property considerations and then predict an effective mixing factor from similar existing experimental data. The other is to use the established fully developed turbulent channel flow result and then attempt to estimate the deviations which would occur in the neighborhood of the channel inlet. Note that although a laminar two-dimensional inlet solution might be useful to indicate the initial level of heating, the subsequent portions of the flow are almost immediately in a transitory state and thus not amenable to a laminar type of behavior.

On the basis of gross properties, the temperature rise times the mass flow would be related to the total heat output as

$$K \dot{m} C_p \Delta T = Q$$

where K is essentially a mixing factor used to relate the actual heat absorbed relative to the total heat capacity of the flow. Therefore the required mass flow can be written

$$\dot{m} = \frac{Q}{K C_p \Delta T}$$

Also by continuity

$$\dot{m} = \rho g \bar{u} A \simeq \rho g \bar{u} \pi d H$$

where d is the mean shroud diameter and H is the distance between the cask wall and shroud.

Next the pressure drop for fully developed turbulent flow in a channel may be approximated as

$$\frac{\Delta p}{L} \quad \frac{H}{\rho \bar{u}^2} = 0.19\,(R_{e_H})^{-1/4}$$

The combination of these three formulas then leads to the result (for the existing cask geometry).

$$\Delta T \quad \Delta P^{4/7} = \frac{0.14}{K\,H^{12/7}} \qquad \begin{array}{l} H \sim \text{ft.} \\ p \sim \text{psi} \end{array}$$

Note however that this Δp only represents the pressure drop in the shroud. In addition there will be a Δp required to attain the basic velocity as

$$\Delta p_u = \frac{\rho \;\bar{u}^2}{2}$$

or

$$\Delta p_u = \frac{\dot{m}^2}{2\,\rho\,g^2\,\pi^2\;d^2 H^2}$$

$$= \frac{1}{2\rho}\left[\frac{Q}{g\,\pi\,d\,H\,K\,C_p\,\Delta T}\right]^2 = \frac{18.0}{(K\,H\;\Delta\;T)^2}$$

Thus the total pressure requirement as a function of the flow temperature rise and effective mixing factor becomes

$$\Delta p_T = \frac{0.032}{H^3\,(K\,\Delta\,T)^{7/4}} + \frac{1.6}{(K\,H\;\Delta\;T)^2}$$

As a typical example, assuming a mixing factor of 0.5, an H of 0.2 inches and a maximum $\triangle T$ of 100 degrees, the total pressure requirement would be

$$\triangle p_T = 8.8 + 2.2$$

$$= 11.0 \text{ psf } (0.076 \text{ psi})$$

and the corresponding mass flow

$$\dot{m} = \frac{1.4}{0.5 \times 0.24 \times 100} = 0.117 \text{ \#/sec}$$

or

$$\dot{m} = 7.0 \text{ \#/min}$$

In selecting a shroud gap, the interference of the supporting structure limits the size to approximately 0.25 inches. Thus for a typical shroud gap of 0.20 inches, the reference level of h would be 16 for an $\dot{m}$ of 20 #/min. and 11. for an $\dot{m}$ of 5 #/min.

Because this shrouded system can be operated at relatively low mass flows, it is necessary to modify the above film coefficient by the net increase in the flow temperature. Since the flow will be turbulent, a total mixing may be assumed so that the flow temperature increase will be

$$\triangle T = \frac{Q}{\dot{m}\, C_p}$$

and will be distributed linearly down the cask. Thus the actual correction will take the form

$$\left[1 - \frac{T_e + \dfrac{Q}{\dot{m}\, C_p} \dfrac{X}{L}}{T_w} \right]$$

so that the modified film coefficient will be

$$h = 0.36 \frac{\dot{m}^{3/4}}{H} \left[1 - \frac{T_e + 5.0 \frac{X}{\dot{m}}}{T_w} \right]$$

where $h \sim BTU/ft^2\ hr\ ^oR$

$\dot{m}$ = mass flow $\sim$ #/sec

T_e = ambient temperature $\sim$ ^oR

T_w = wall temperature $\sim$ ^oR

H = shroud gap $\sim$ feet

X = cylinder distance $\sim$ feet

The alternate form of shroud analysis is based on an attempt to predict the local wall shear in a channel inlet and then to use the Reynolds analogy to convert this result to an effective heat transfer. While plots of the experimentally established values of skin friction versus Reynolds number for turbulent parallel flow in a channel are available, the form of the resulting curve fit is rather unwieldy for use in additional derivations. Therefore the approximate form as

$$C_{f/2} = 0.10\ (R_{e_h})^{-1/4}$$

where $C_{f/2}$ here represents the skin friction on only one side of the channel wall. Thus the Stanton number would be

$$St \simeq \frac{0.10}{P_r^{\ 2/3}}\ (R_{e_h})^{-1/4}$$

$$= 0.12\ (R_{e_h})^{-1/4}$$

and the film coefficient

$$h = 2.2 \times 10^{-3}\ \bar{u}/(R_{e_h})^{1/4}$$

Through the continuity equation, this equation may be rewritten (for relatively small values of the shroud gap and for the particular cask geometry)

$$h = 0.36 \ \frac{\dot{m}^{3/4}}{H}$$

where

$\dot{m} \sim$ #/sec.

$H \sim$ ft.

5.2 Cross Flow Cooling Systems (Drawing 5)

The basic objective behind this type of design is to attain an essentially uniform temperature distribution across the flow. If this objective can be met, then the subsequent mass flow requirement will be considerably less than that of the other cooling systems.

The flow mixing which will be necessary to achieve a uniform temperature distribution will be derived from two sources; 1. The maintenance of turbulent flow between the walls, and 2. The maintenance of the Goertler vortices which will exist in the flow between concentric cylinders at the required Reynolds numbers for turbulent flow. The existence of such mixing will not allow any significant temperature gradients in the flow. Thus this type of shroud may be analyzed on the basis of the total heat content of the flow rather than on any local boundary layer theory. However it will be necessary to maintain some temperature difference between the cask wall and the air flow so that there will be a net heat transfer, i.e., it cannot be expected to use just enough mass flow so that the exit air is at the same temperature as the cask wall.

The basic method of analysis of this type of shroud is to first estimate the streamline pattern. Then through two-dimensional channel flow analysis, the mean velocity may be calculated as a function of the mass flow, channel width, and available pressure differential. As the cask heat output is known and the temperature gradient across the flow is assumed to be zero, the net temperature rise in the flow may be related to the mass flow and subsequently to the available pressure drop. It then only remains to check that the Reynolds numbers are adequate to maintain turbulent flow between the cylinder walls. The essentials of this analysis are given below.

The net heat output of the cask is 1500 watts or 1.4 BTU/sec. Thus the required mass flux in terms of a temperature rise is:

$$\dot{m}_{req}\ C_p\ \Delta T = Q$$

or

$$\dot{m}_{req} = \frac{336}{\Delta T}. \qquad (\dot{m} \sim \#/\text{min})$$

By continuity the mass flux may be related to the velocity as

$$\dot{m} = \rho g UA$$

where A is the effective cross sectional area of the entering flow. Thus the velocity may be related to the temperature rise as:

$$\overline{U} = \frac{336}{\rho g A \Delta T}$$

For turbulent flow between parallel plates (channel flow) the pressure drop may be written

$$\frac{dp}{dx} = 0.11\ \frac{\rho \overline{U}^2}{H} \left(\frac{\overline{U}H}{v}\right)^{-1/4}$$

where H is the height of the channel.

If the ratio of the effective channel width to the channel height is defined as n, then the effective area, A, will be nH^2 and the above equations can be combined to yield:

$$\Delta p \Delta T^{7/4} = \frac{0.135}{n^{11/4}\ H^{23/4}}$$

As a sample case, the presently proposed configuration has an n of approximately 6 and an H of 0.037 feet. ΔT was arbitrarily selected as 100°R and thus:

$$\Delta p = \frac{0.135}{6^{2.75}\ (037)^{5.75} \times (100)^{1.75}} = 50 \text{ psf or } 0.35 \text{ psi}$$

also $$\dot{m} = \frac{336}{100} = 3.4 \quad \#/\text{min}$$

and $$\bar{u} = \frac{336}{0.076 \times 6 \times (1.37)^2 \times 100} = 90 \text{ fps}$$

so that the Reynolds number will be:

$$R_e = \frac{UH}{v} = \frac{90 \times 0.037}{1.65 \times 10^{-4}} = 13,500$$

which is well above the level required to maintain turbulent flow.

An additional pressure drop will be required to accelerate the flow to the given velocity as

$$p_1 - p_2 = \frac{\rho \bar{u}^2}{2}$$

or

$$\Delta p_u = \frac{\rho \bar{u}^2}{2} = \frac{0.002378(90)^2}{2}$$

$$= 9.6 \text{ psf} = 0.07 \text{ psi}$$

Thus the total pressure drop of the system will be

$$\Delta p_{total} = 0.35 + 0.07 = 0.42 \text{ psi}$$

Since the thermodynamic analysis requires a film coefficient, it is necessary to establish the local heat transfer- even though the system is adequately analyzed on a gross basis. To determine the local film coefficient, the wall temperature is applied to the heat transfer as:

$$\dot{q} = \dot{q}_o \left[1 - \frac{T_e}{T_w} \right]$$

where T_e is the effective boundary layer temperature. Since it has been assumed that there is total mixing, the local temperature rise may be written as:

$$\dot{m}\, C_p\, \Delta T = 2\pi R \int_o^x \dot{q}\, dx$$

or

$$\Delta T = \frac{2\pi R \dot{q}}{\dot{m}\, C_p} \quad x$$

Assuming an ambient temperature of 80^{o}F and a cask wall temperature of 340^{o}F, this heat transfer (and thus film coefficient) correction will be

$$h = h_o \left[1 - \frac{540 + \frac{2\pi R\dot{q}}{\dot{m}\, C_p} x}{800} \right]$$

Since the correction is linear the average value of h (as calculated from the first part) and the local value of h will be equal at a point halfway along the cask - thereby furnishing a means for calculating the reference value of h_o. i. e.,

$$h_{avg} = \frac{Q}{A \Delta T} = \frac{\dot{m}\, C_p}{A}$$

thus at x = L/2

$$h_o = \frac{h_{avg}}{\left[1 - \frac{540 + \frac{2\pi R\dot{q}}{\dot{m}\, C_p} L/2}{800} \right]}$$

Consequently for the example given above,

$$h_o = 77 \text{ BTU/ft}^2 \text{ HR } ^oR$$

which gives a linear distribution of h from a value of

$$h = 25 \text{ BTU/ft}^2 \text{ HR } ^oR$$

at the beginning of the flow, to a value of

$$h = 15 \text{ BTU/ft}^2 \text{ HR } ^\circ\text{R}$$

at the opposite end of the cooling shroud.

5.3 Normal Flow Cooling Systems (Fig. 5.1)

The internal liner of the shroud has appropriately distributed holes so that the cooling mechanism is essentially a series of stagnation region flows on the cask. For purposes of analysis the individual stagnation flow regimes must then be modified to incorporate the cross flow which exists and increases towards the ends of the shroud.

As the distance between the shroud and the cask wall is increased the cross flow velocity is reduced, thereby decreasing the asymmetric effect upon the local impingement solutions. However the geometric restrictions of the mounting hardware have reduced the allowable separation distance to a point where the cross flow in the neighborhood of the shroud ends is a significant contributor to the overall cooling. This effect in itself is not undesirable, but in the center section of the shroud where there is little or no cross flow cooling, the direct flow impingement cooling is not operating at its most efficient configuration. Also the cooling should be greatest at the center since the end cooling is already aided by internal axial conduction through the end caps of the cask. To some extent this problem can be compensated for by non-uniform placement of the shroud cooling holes, but the required iterative analysis becomes much more complicated.

For convenience on the preliminary analysis, it is assumed that the stagnation and cross flow solutions are linear, i.e., may be superimposed upon each other. The basic procedure is to develop a local stagnation region flow solution and then integrate it over the effective area covered so that an average film coefficient may be established as a function of an increment of area. With this formulation and the available pressure and mass flow of coolant, it is possible to specify the number of holes in the shroud as a function of the average value of the film coefficient. A typical example is carried out below.

NORMAL FLOW OPEN SHROUD PURGE SYSTEM

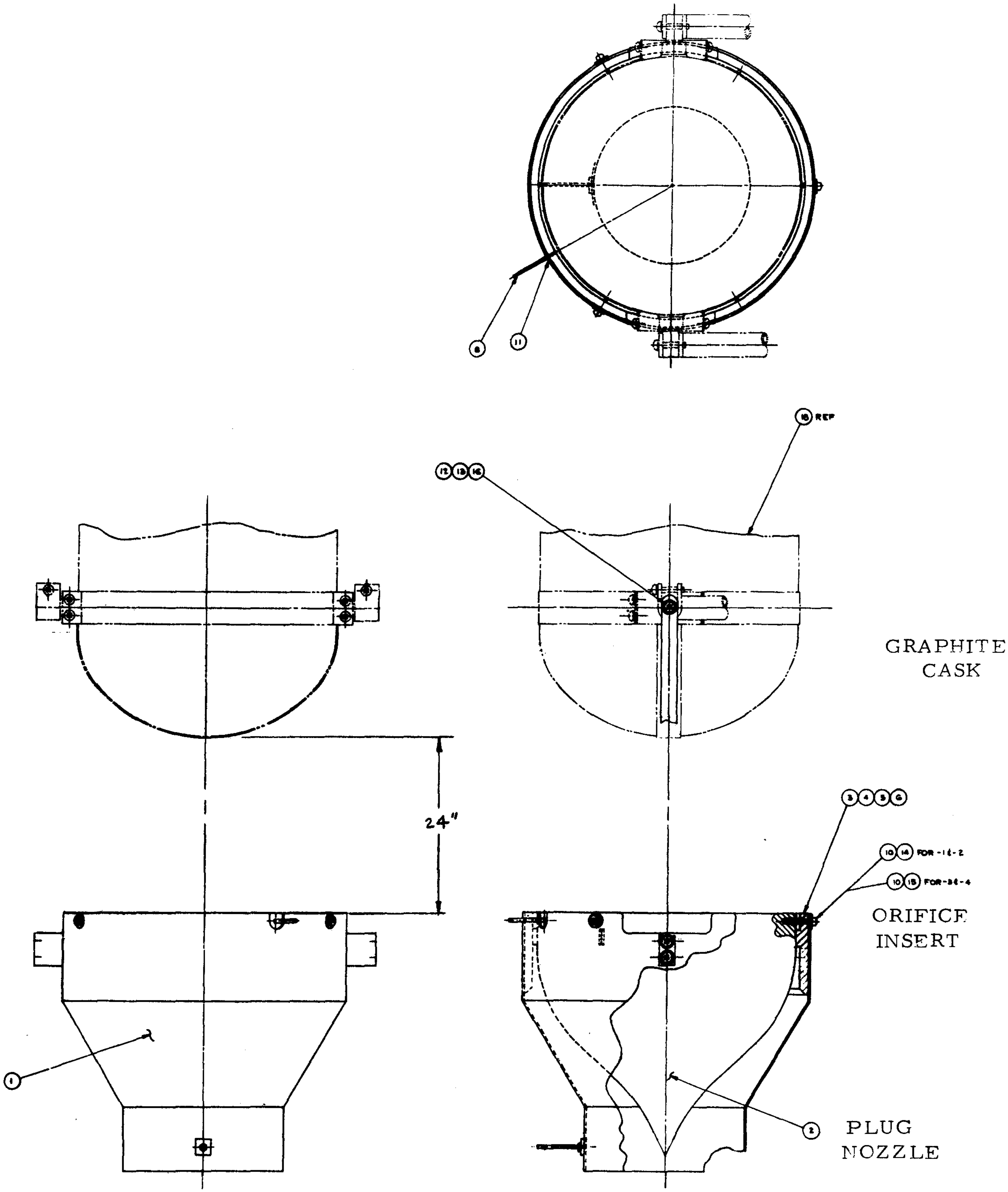

Figure 5.1

From volume 5 of the Princeton Series the Stanton number for flow normal to a cylinder is given as:

$$St = 0.57 \left(\frac{C_p \mu}{K} \right)^{-.6} \left(\frac{BD}{U} \right)^{0.5} (R_{e_D})^{-0.5}$$

where for a cylinder of diameter D, BD/U = 4.0.

Thus for a Prandtl number of 0.71 for air,

$$St_{cyl} = 1.4 / \sqrt{R_{e_D}}$$

Because of the relatively small distance between the holes and the wall (the order of several hole diameters) the effective exit velocity may be used in the stagnation point solution i.e., there will be very little velocity decay in such a short distance. Note however that the stagnation velocity is somewhat fictitious in that it does not actually exist at the stagnation point.

Using the definition of the film coefficient as:

$$h \equiv \frac{q}{\Delta T} = \rho \, g \, U \, C_p \, St$$

the stagnation point film coefficient becomes

$$h = \frac{0.25}{\sqrt{R_{e_D}}} \; C_D \sqrt{\frac{2 \Delta p}{\rho}}$$

However since it is the stagnation region rather than the stagnation point which is of interest, this relation must be modified to be a function of r (the radial surface distance from the geometrical stagnation point). Basically this local value of h may be obtained by multiplying the stagnation value of h by the local velocity ratio. This velocity ratio as a function of r may be obtained from the momentum and continuity equations, but since the functional form is not simple and since it must be integrated to yield an average value of h as a function of r (or actually the effective surface area) it will be necessary to resort to a graphical means of solution.

In the table below the local and integrated average values of the film coefficient are given as a function of the ratio of the exit diameter to the surface radius.

d/r	h'/h_{st}	$\bar{h}/h_{st}$	A/A_{ex}
0	1	1	0
1/2	0.7	0.77	16
1/4	0.5	0.60	64
1/6	0.41	0.51	144
1/8	0.35	0.45	256
1/12	0.29	0.38	576

where $\bar{h}/h_{st} = \frac{2\pi}{\pi r^2} \int h'/h_{st}\, r\, dr$

Assuming that the available pressure differential would be 1 psi and the hole diameter to be 1/8 inch, then the values of h_{st} and A_{ex} are specified. Then the number of holes required and the resultant mass flow as a function of h may be obtained as

$$\text{number of holes} = n = \frac{A_{total}}{\Delta A}$$

$$\text{mass flux} = m = \rho g\, U_{ex} A_{ex}$$

and these values are given in the table below (with $A_{total} \simeq 350$ sq. in.)

h (BTU/ft^2 $^\circ$R HR)	h (no. 1/8" dia. holes)	m (#/min)	$V_{exhaust}$
15	--	∞	--
11.6	1750	163	200
9.0	440	42	53
7.7	200	19	24
6.8	110	10	13
5.7	50	4.6	5.7

Next it is necessary to establish the heat transfer corrections for the cross flow and the increase in the boundary layer temperature as the flow proceeds from the center section to the ends of the shroud. Assuming a 1/2 inch gap between the shroud and cask wall, the exhaust velocity at the ends of the shroud are given in the above table.

If the cask heat output is uniform, then the new heat added at any point along the cask will be

$$\int_o^x \dot{q}\, dx = \dot{q}x$$

where x has its origin at the middle.

The accompanying temperature rise from this heat addition would be

$$\dot{m}' C_p \Delta T \gamma' = \int \dot{q}dx = \dot{q}x$$

where $\dot{m}'$ is the mass added from the centerline up to point x and γ' is the mixing ratio, i.e., the proportion of the total flow which is actually heated. Then as $\dot{m} = \dot{m}_T$ (L/2) X, the temperature rise would be:

$$T = \frac{2\dot{q}}{\gamma' C_p L \dot{m}_T}$$

and thus is independent of x. Further the nominal values of ΔT for a mixing factor of approximately 0.5 and the relatively low mass flow of 20 #/min would be only 24^{o}R. Consequently the boundary temperature correction would be at most a second order one. Also from the above table it may be noted that the end exhaust velocity for the mass flux of 20 #/min is approximately 25 fps. Such a velocity would not yield a significant increase in the film coefficient. Therefore since these two effects (flow temperature rise and cross flow) are small and act in opposite directions, they may properly be considered small and self-canceling for the realistic levels of open shroud cask cooling.

5.4 Water Cooling Systems

Water systems have been studied for the on-pad cooling of the RTG cask. Two water cooling systems have been considered; a closed system which removes the heat by a temperature rise of the water and an open system which removes the heat by boiling off water. The individual systems and thermal analysis are described in the following paragraphs.

The RTG cask is an eight inch diameter cylinder with spherical dome ends and has an overall length of 23 inches. The dome ends are insulated and the primary heat rejecting surface is the center portion of the cask. This cylindrical surface is 14.25 inches long and has an 8 inch diameter for a rejecting area of 2.5 square feet. This cask is held by a tubular frame to the LEM vehicle and limited space is available between the cask and frame for the water jacket hardware. For purposes of analysis, a water jacket thickness of 0.25 inches and a length of 14 inches were established. Heat is released at a rate of 5120 BTU/hr from the cask and is absorbed by the water in the cooling jacket.

The volume of the water jacket is 0.054 cubic feet and has a capacity for holding 3.37 pounds of water. If cooling water is available at 60°F, the necessary flow rate of water with a 100°F temperature rise to remove the heat is

$$\dot{w} = \frac{q}{C_p \Delta T} = \frac{5120}{(0.99)(100)(60)} = 0.86 \text{ lbm/min}$$

where q = heat absorbed, 5120 BTU/hr

C_p = specific heat, 0.99 BTU/lbm $^{\circ}$F

ΔT = temperature rise, 100°F.

The entering water requires time to pick up the heat and pass through the jacket. This time is obtained by the following calculation,

$$\frac{\text{Capacity}}{\text{flow rate}} = \frac{3.37}{0.86} = 3.9 \text{ minutes.}$$

5.4.1 Closed System

In the thermal analysis, there are three approaches with which to look at the water jacket cooling system and establish the heat transfer film coefficient. These approaches are free convection, forced convection and conduction; however none of these methods provide individually a true model of the actual situation. The thin layer of water around the cask does not allow the natural circulation currents to develop as in free convection and also a steady supply of cool water is introduced which affects the circulation currents. Likewise the inflow velocity of cool water is low and cannot provide good conditions for forced convection. In the conduction approach, the water is assumed as a solid material and heat is conducted from the cask to the water, as the water is slowly moved through the jacket. Thus the water serves as a heat sink and is discarded when warmed up. An analysis is made for each approach and the resulting film coefficients are compared.

The free convection analysis is based on correlation data for vertical plates and cylinders heat transfer studies. This correlation data is plotted as a function of Grashof (Gr), Prandtl (Pr), and Nusselt (Nu) numbers for the laminar, transition and turbulent flow ranges. For three-dimensional shapes, a characteristic length, L, is determined by

$$\frac{1}{L} = \frac{1}{L\ \text{hor.}} + \frac{1}{L\ \text{vert.}}$$

where L hor. = average horizontal dimension

L vert. = height dimension

Therefore, the characteristic length is

$$\frac{1}{L} = \frac{1}{8} + \frac{1}{14} = \frac{11}{56}$$

or

$$L = \frac{56}{11} = 5.1 \text{ inches}$$

The product of Gr and Pr is

$$Gr\ Pr = \left[\frac{g\, P^2 \beta}{N^2} \quad L^3 \Delta T\right]\left[\frac{C_p\, \mu}{k}\right]$$

where

g = acceleration of gravity

β = temperature coefficient of volume expansion

ρ = density

μ = absolute viscosity

L = characteristic length

ΔT = temperature difference between surface and water, $27^\circ F$

Cp = specific heat

k = thermal conductivity

Substitution of values for water at $100^\circ F$ gives

$$Gr\ Pr = (118 \times 10^6) \left(\frac{5.1}{12}\right)^3 \quad (27)\ (4.52) = 1.11 \times 10^9$$

This value for the Gr Pr product is at the beginning of the turbulent flow range and the following relationship holds

$$Nu = 0.021\ (GrPr)^{2/5}$$

Therefore

$$Nu = 0.021\ (1.11 \times 10^9)^{2/5} = 87.2$$

The Nusselt number is defined by this expression

$$Nu = \frac{hL}{k}$$

where

h = heat transfer coefficient

L = characteristic length

k = thermal conductivity

Now

$$h = \frac{k}{L} \quad Nu = \frac{0.364\ (12)}{5.1} \qquad (87.2)$$

$$h = 75\ BTU/hr\ ft^2\ {}^{o}F$$

The heat rejected by free convection is

$$q = A\ h \Delta T$$

$$q = (2.5)\ (75)\ (27) = 5060\ BTU/hr.$$

The forced convection thermal analysis is based on the flow conditions of the water in the jacket surrounding the fuel cask. Laminar flow exists for a Reynolds (Re) number below 2100. For the water jacket, the hydraulic diameter, D_H, is

$$D_H = D_2 - D_1$$

where the subscript 2 denotes the outer diameter of the water jacket and subscript 1 is the inner diameter. Therefore,

$$D_H = 8.5 - 8.0 = 0.5 \text{ inches}$$

The cross-sectional flow area is

$$A = \frac{\pi}{4} \quad (D_2{}^2 = D_1{}^2)$$

$$= \frac{\pi}{4} \quad (8.25) = 6.48 \text{ sq. in.}$$

Now the velocity, V, is determined from the expression,

$$V = \frac{\dot{w}}{\rho A}$$

where $\dot{w}$ = water flow rate, 0.86 lbm/min

ρ = water density, 62.2 lbm/ft^3

A = flow area, 6.48 sq. in.

With these values, the velocity is

$$V = \frac{0.86\ (144)}{62.2\ (6.48)\ (60)} = 0.0051 \text{ fps}$$

The Reynolds number becomes

$$R_{eD} = \frac{V\ D_H\ \rho}{\mu} = \frac{(0.0051)\ (0.5)\ (62.2)}{(0.458 \times 10^{-3})\ (12)} = 28.9$$

and therefore the flow is definitely laminar through the water jacket.

The heat transfer coefficient for laminar flow is based on the empirical equation which correlates experimental results for liquids. This equation has the form:

$$Nu = 1.86 \left[\frac{R_{eD}\ Pr\ D}{L}\right]^{0.33} \left(\frac{\mu_b}{\mu_s}\right)^{0.14}$$

where the correction factor $(\mu_b/\mu_s)^{0.14}$ accounts for the temperature variation effects on the physical properties. Substitution of values into equation (11) gives a value of

$$Nu = 1.86 \left[\frac{(28.9)\ (4.52)\ (0.5)}{5.1}\right]^{0.33} \left(\frac{0.458 \times 10^{-3}}{0.292 \times 10^{-3}}\right)^{0.14}$$

$$Nu = 4.59$$

Then the heat transfer coefficient is

$$h = \frac{k}{L} \text{ Nu} = \frac{0.364\ (12)\ (4.59)}{5.1} = 3.92 \text{ BTU/hr ft}^2\ {}^\circ\text{F}$$

The water flow rate of 0.86 pounds per minute requires a 100°F temperature rise of the water and an average temperature of 110°F. If the cask surface temperature is 210°F, then a 100°F temperature differential exists and the heat transferred is

$$q = AR\ \Delta T$$

$$= (2.5)\ (3.92)\ (100) = 980 \text{ BTU/hr.}$$

A third approach with which to analyze the closed water cooling system is by conduction from the cask into the water. The water jacket thickness of 0.25 inches is very small compared to the cask radius and therefore the cask surface and the water jacket are considered parallel flat surfaces. The heat transfer conduction equation has the following form

$$q = \frac{k}{L}\ A\ \Delta T$$

where k = thermal conductivity of water, 0.364 BTU/hr ft °F

L = length of conduction path, 0.125/12 feet

A = cross sectional area,

Thus the term k/L is similar to the film coefficient h, and has the same units. This term has the value of

$$\frac{k}{L} = \frac{0.364\ (12)}{0.125} = 35 \text{ BTU/hr ft}^2\ {}^\circ\text{F}$$

The necessary temperature difference to remove the heat is

$$\Delta T = \frac{q}{A\left(\frac{k}{L}\right)} = \frac{5120}{2.5\ (25)} = 59^\circ\text{F}.$$

In the three thermal analysis approaches, the heat transfer film coefficients were determined as i for free convection - 75 BTU/hr ft^2 ^oF, for forced convection - 3.92 and for conduction - 35. The free convection and conduction approaches best fit the physical conditions of this problem even though there is a slow flow of water through the jacket. A conservative film coefficient is the 35 BTU/hr ft ^oF from the conduction analysis and the actual film coefficient value is determined from the experimental tests of this cooling system concept.

The temperature differential between a particular point on the cask surface and the water is determined from equation (12). But the temperature is expected to vary along the axis of the cask as the water temperature increases from the inlet. For the above system a temperature drop exists across the inner wall of the water jacket which was not determined in these calculations but the temperature is the same for all the above approaches.

5.4.2 Open System

The open system has the same sized water jacket as in the closed system but water is boiled off to remove the heat from the RTG cask. The water level is maintained high on the cask by a flow rate equal to the boil-off rate. In the open system the boiling temperature is 212^oF and the water enters at 60^oF; therefore some of the cask heat raises the water temperature to the boiling point and the remainder of the heat vaporizes the water. The flow rate of water is determined by

$$\dot{w} = \frac{q}{c_p \Delta T + h_{fg}}$$

where $\dot{w}$ = water flow rate, lbm/hr

q = heat to be rejected, 5120 BTU/hr

c_p = specific heat of water, 0.99 BTU/lbm - ^oF

ΔT = temperature use of water, (212-60) = 152^oF

h_{fg} = latent heat of vaporization, 97^o BTU/lbm

with the above values, the flow rate is 4.57 lbm/hr.

The nature of the boiling is a complex phenomena and is dependent on many variables. An excess temperature, ΔT_x, is the difference between the hot surface and fluid saturation temperature. This excess temperature and the heat flux of the surface determine the boiling regime of open water cooling system. The expected temperature excess of this system is small and the heat flux is 2045 BTU/hr - ft^2 which indicates a pool boiling regime. An empirical relationship between the excess temperature, heat flux and physical variables is

$$\frac{c_\ell \; \Delta T_x}{h_{fg} \; Pr_\ell^{1.7}} = C_{sf} \left[\frac{q/A}{\mu_\ell \; h_{fg}} \sqrt{\frac{g_c \; \sigma}{g \, (\rho_\ell - \rho_v)}} \right]^{0.33}$$

where

c_ℓ = specific heat of saturated liquid, 1 BTU/lbm $^\circ$F

q/A = heat flux, 2045 BTU/hr ft^2

h_{fg} = latent heat of vaporization, 970 BTU/lbm

g_c = conversion factor, 4.17×10^8 lbm ft/lbf hr^2

g = gravitational acceleration, 4.17×10^8 ft/sec^2

ρ_ℓ = density of saturated liquid, 59.97 lbm/ft^3

ρ_v = density of saturated vapor, 0.0372 lbm/ft^2

σ = surface tension of the liquid-to-vapor interface, 4.98×10^{-3} lbf/ft

Pr_ℓ = Prandtl number of the saturated liquid, 1.74

μ_ℓ = viscosity of the liquid, 0.205×10^{-3} lbm/ft-sec

C_{sf} = empirical constant depending on the nature of the heating surface - fluid combination, 0.01.

(Reference for equation: "Principles of Heat Transfer," F. Krieth, p. 406). The excess temperature is 7.5°F for the above listed values and therefore the surface temperature is approximately 220°F. The pool boiling heat-transfer coefficient, h_b, is defined by

$$h_b = \frac{q/A}{\Delta T_x}$$

and has the value of 273 BTU/hr ft^2 - ^oF.

Therefore the thermal analysis has shown that both the closed and open water systems are capable of holding the RTG cask at or below a temperature of 220^{o}F.

5.5 Cask Shroud Removal Investigation

Although the concept of a shrouded cask cooling system represents a highly efficient approach to the problem, it also presents an interference problem to the radiation cooling of the cask on the later portions of the flight. Therefore it is necessary to include some form of removal of the shroud in the total system design. The two removal techniques which were considered in this analysis were that of post launch mechanical removal or post launch self destruct of the shroud.

The problems encountered in the mechanical removal of the shroud were the many degrees of freedom required of the shroud to clear the cask mounting hardware. For a rigid shroud it appears that at least three separate pieces plus a mechanical release system (probably thermally actuated) would be required to be able to pull such a shroud away from the cask. In addition these mechanical withdrawal links (springs, etc.) would have to be oriented in different positions. Consequently the high complexity and probably weight penalty of such a removal system led to the consideration of the second type of system, i.e., the self-destructing system.

Once the cooling GN2 system has been shut down in the post launch sequence, the heat output of the RTG cask will increase the shroud temperature (by radiation heating). Therefore a material is required which is structurally sound at the shroud temperature during cooling and which will decompose at an elevated temperature without damaging the cask and its contents.

The actual form of the decomposition could be that of melting, charring, or subliming. However for melting, such as would be attained with a thermoplastic, the subsequent deposition of material presents a problem. On the other hand most subliming materials contain highly reactive chemical constituents such as fluorine which could attack the cask surface, etc. Therefore the charring materials appear to present the most attractive approach. Such materials as certain phenolics decompose in the proper temperature range (300° - 400°) and with the proper filler result in an end product of only a fine ash. The only real question is the actual time of decomposition in the anticipated environment. If this time were too large, there could be significant overshoot in the cask temperature above that of the equilibrium space radiation temperature. Such a temperature overshoot would increase the decomposition rate, but this type of interaction would require careful study to insure capsule integrity throughout the shroud removal sequence.

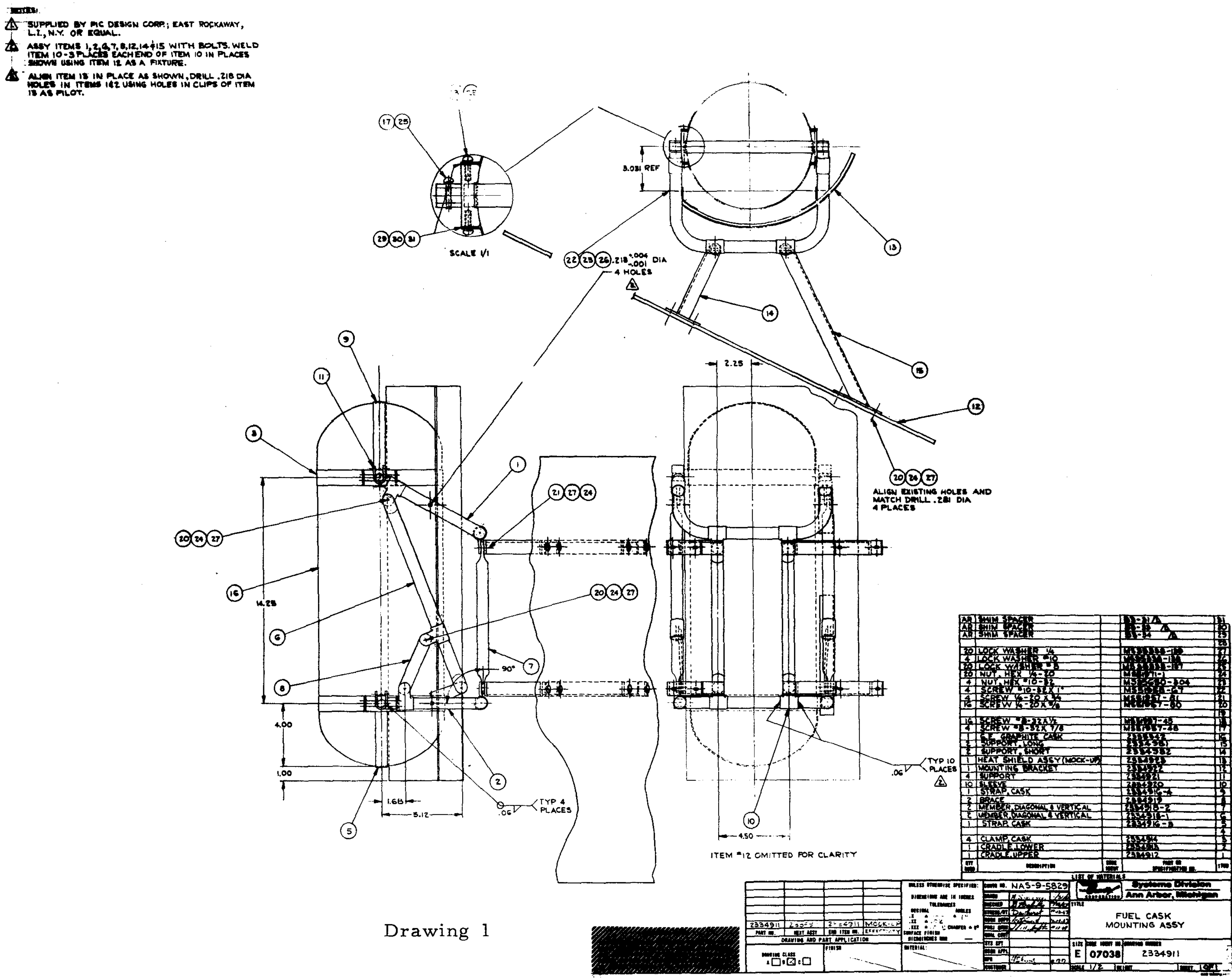

NOTES:
1 SUPPLIED BY PIC DESIGN CORP.; EAST ROCKAWAY, L.I., N.Y. OR EQUAL.
2 ASSY ITEMS 1,2,6,7,8,12,14 & 15 WITH BOLTS. WELD ITEM 10-3 PLACES EACH END OF ITEM 10 IN PLACES SHOWN USING ITEM 12 AS A FIXTURE.
3 ALIGN ITEM 13 IN PLACE AS SHOWN, DRILL .218 DIA HOLES IN ITEMS 1&2 USING HOLES IN CLIPS OF ITEM 13 AS PILOT.
SCALE 1/1
3.031 REF
.218 +.004 -.001 DIA 4 HOLES
ALIGN EXISTING HOLES AND MATCH DRILL .281 DIA 4 PLACES
2.25
4.50
14.25
4.00
1.00
1.68
5.12
90°
.06
TYP 4 PLACES
TYP 10 PLACES
ITEM #12 OMITTED FOR CLARITY
AR SHIM SPACER
AR SHIM SPACER
AR SHIM SPACER
20 LOCK WASHER 1/4
4 LOCK WASHER #10
20 LOCK WASHER #8
20 NUT, HEX 1/4-20
4 NUT, HEX #10-32
4 SCREW #10-32 X 1"
4 SCREW 1/4-20 X 3/4
16 SCREW 1/4-20 X 5/8
16 SCREW #8-32 X 1/2
4 SCREW #8-32 X 7/8
1 G.E. GRAPHITE CASK
2 SUPPORT, LONG 2334961
2 SUPPORT, SHORT 2334982
1 HEAT SHIELD ASSY (MOCK-UP) 2334923
1 MOUNTING BRACKET 2334922
4 SUPPORT 2334921
10 SLEEVE 2334920
1 STRAP, CASK 2334916-4
2 BRACE 2334919
2 MEMBER, DIAGONAL & VERTICAL 2334918-2
2 MEMBER, DIAGONAL & VERTICAL 2334918-1
1 STRAP, CASK 2334916-3
4 CLAMP, CASK 2334914
1 CRADLE, LOWER 2334913
1 CRADLE, UPPER 2334912
LIST OF MATERIALS
NAS-9-5829
Systems Division
Ann Arbor, Michigan
FUEL CASK
MOUNTING ASSY
E 07038 2334911
2334911

Drawing 1

NOTES:
⚠1 THIS ASSEMBL. SHALL BE ONE BASIC UNIT WITH INTERCHANGEABLE SLEEVES, ITEMS 3 THRU 6. THE ONLY VARIATION BETWEEN DASH NUMBERS ARE THE SLEEVES THEMSELVES AND THE HARDWARE REQUIRED FOR SECURING THEM.

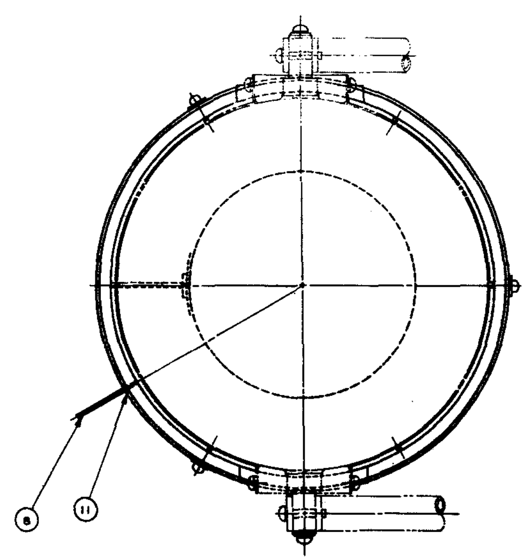

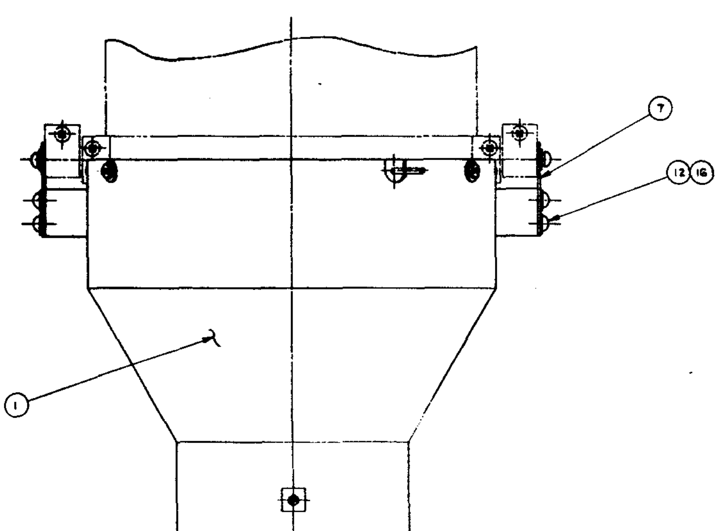

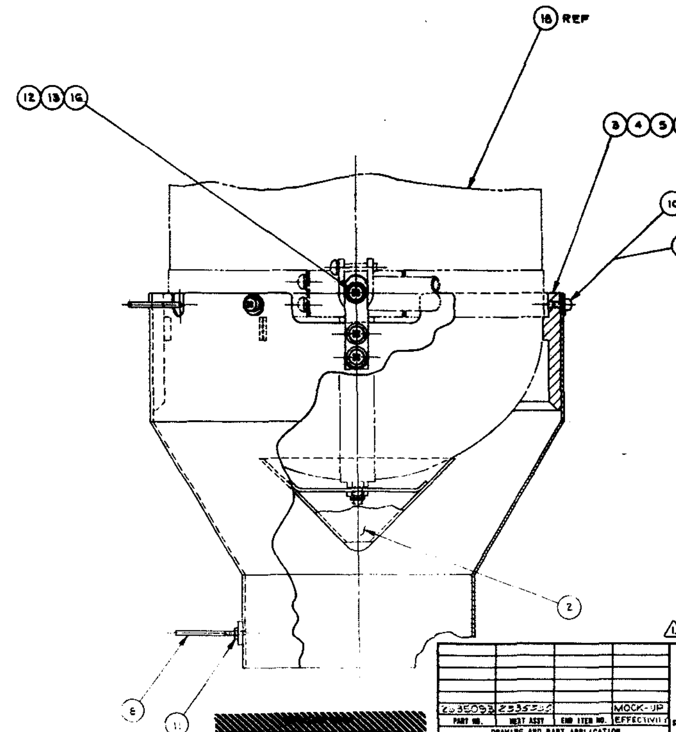

Drawing 2

QTY REQD -4	QTY REQD -3	QTY REQD -2	QTY REQD -1	DESCRIPTION	CODE IDENT	PART OR SPECIFICATION NO.	ITEM
							19
REF	REF	REF	REF	FUEL CASK MTG ASSY		[redacted]	18
							17
6	6	6	6	WASHER, FLAT #8		MS1[redacted]-807	16
3	3	—	—	SCREW, PAN HD, THD FORMING (#6 X .25)		MS2[redacted]-16	15
—	—	3	3	SCREW, PAN HD (#6-32 X .25)		M[redacted]-26	14
2	2	2	2	LOCK WASHER #8		MS[redacted]-80	13
6	6	6	6	SCREW #8-32 X 1/2		M[redacted]-45	12
2	2	2	2	NUT, HEX #2-56		M[redacted]-224	11
3	3	3	3	WASHER, FLAT #6		MS15795-806	10
							9
2	2	2	2	TUBE, MODIFIED		[redacted]	8
2	2	2	2	HANGER		[redacted]	7
1	—	—	—	SLEEVE, THIN WALL		[redacted]	6
—	1	—	—	SLEEVE, THIN WALL		[redacted]	5
—	—	1	—	SLEEVE, HEAVY WALL		[redacted]	4
—	—	—	1	SLEEVE, HEAVY WALL		[redacted]	3
1	1	1	1	AIR DIRECTING CONE		[redacted]	2
1	1	1	1	AIR COOLING CONE		[redacted]	1

LIST OF MATERIALS

2835093	2835555		MOCK-UP
PART NO.	NEXT ASSY	END ITEM NO.	EFFECTIVITY

DRAWING AND PART APPLICATION

DRAWING CLASS A ☐ B ☒ C ☐

FINISH

UNLESS OTHERWISE SPECIFIED: DIMENSIONS ARE IN INCHES
TOLERANCES
DECIMAL .X ± .XX ± .XXX ±
ANGLES ±
CHAMFER ± 0°
SURFACE FINISH MICROINCHES RMS

MATERIAL:

CONTR NO. NAS 9-5829		
DRAWN	R. KALLERMAN	10/10/67
CHECKED	Lewinski	11/27/67
STRESS/WT		
DSGN SUPV		
PROJ ENGR		
QUAL CONT		
SYS SPT		
DSGN APPL		
MFG		
CUSTOMER		

Bendix Corporation — Systems Division, Ann Arbor, Michigan

TITLE: AXIAL FLOW PURGE SYSTEM ASSY

SIZE E | CODE IDENT NO. 07038 | DRAWING NUMBER 2835093

SCALE FULL | WEIGHT | SHEET 1 OF 1

NOTES:

1. THIS ASSEMBLY SHALL BE ON UNIT WITH INTERCHANGEABLE SLEEV EMS 3 THRU 6. THE ONLY VARIATION BETWEEN DASH NUMBERS ARE THE SLEEVES THEMSELVES AND THE HARDWARE REQUIRED FOR SECURING THEM.

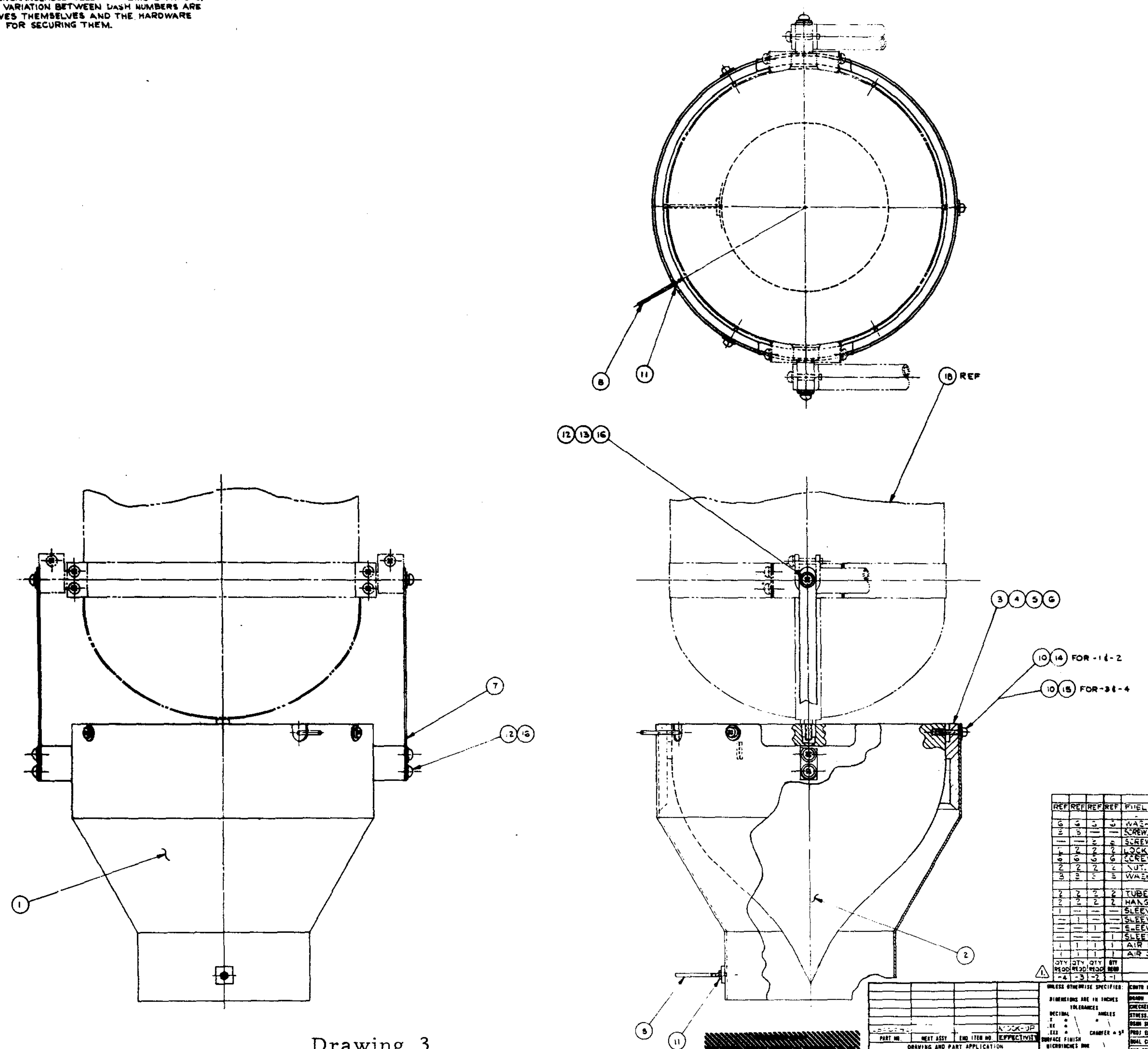

Drawing 3

-4 QTY REQD	-3 QTY REQD	-2 QTY REQD	-1 QTY REQD	DESCRIPTION	CODE IDENT	PART OR SPECIFICATION NO	ITEM
							19
REF	REF	REF	REF	FUEL CASK MTG ASSY		2334911	18
							17
6	6	3	3	WASHER, FLAT #8		MS15795-807	16
3	3	—	—	SCREW, PAN HD, THD FORMING (#6 X .75)		MS24618-21	15
—	—	3	3	SCREW, PAN HD (#6-32 X .75)		MS51957-32	14
2	2	2	2	LOCK WASHER #8		MS35338-80	13
6	6	6	6	SCREW #8-32 X 3/8		MS51957-43	12
2	2	2	2	NUT, HEX #2-56		MS35649-224	11
3	3	3	3	WASHER, FLAT #6		MS15795-806	10
							9
2	2	2	2	TUBE, MODIFIED		2335304	8
2	2	2	2	HANGER, LONG		2335845	7
1	—	—	—	SLEEVE, THIN WALL		2335097-7	6
—	1	—	—	SLEEVE, THIN WALL		2335097-6	5
—	—	1	—	SLEEVE, HEAVY WALL		2335096-6	4
—	—	—	1	SLEEVE, HEAVY WALL		2335096-5	3
1	1	1	1	AIR DIRECTING CONE NO. 2		2335844	2
1	1	1	1	AIR COOLING CONE		2335094	1

LIST OF MATERIALS

PART NO.	NEXT ASSY	END ITEM NO.	EFFECTIVITY
			MOCK-UP

DRAWING AND PART APPLICATION

DRAWING CLASS A ☐ B ☒ C ☐

FINISH

UNLESS OTHERWISE SPECIFIED: DIMENSIONS ARE IN INCHES
TOLERANCES
DECIMAL .X ± .XX ± .XXX ±
ANGLES ±
CHAMFER ± 3°
SURFACE FINISH MICROINCHES RMS

MATERIAL:

CONTR NO. NAS 9-5829

DRAWN R. KELLERMAN
CHECKED
STRESS/WT
DSGN SUPV
PROJ ENGR
QUAL CONT
SYS SPT
DSGN APPL
MFG
CUSTOMER

The Bendix Corporation Systems Division Ann Arbor, Michigan

TITLE AXIAL FLOW PURGE SYSTEM ASSY NO. 2

SIZE E | CODE IDENT NO. 07038 | DRAWING NUMBER 2335343

SCALE FULL | WEIGHT | SHEET 1 OF 1

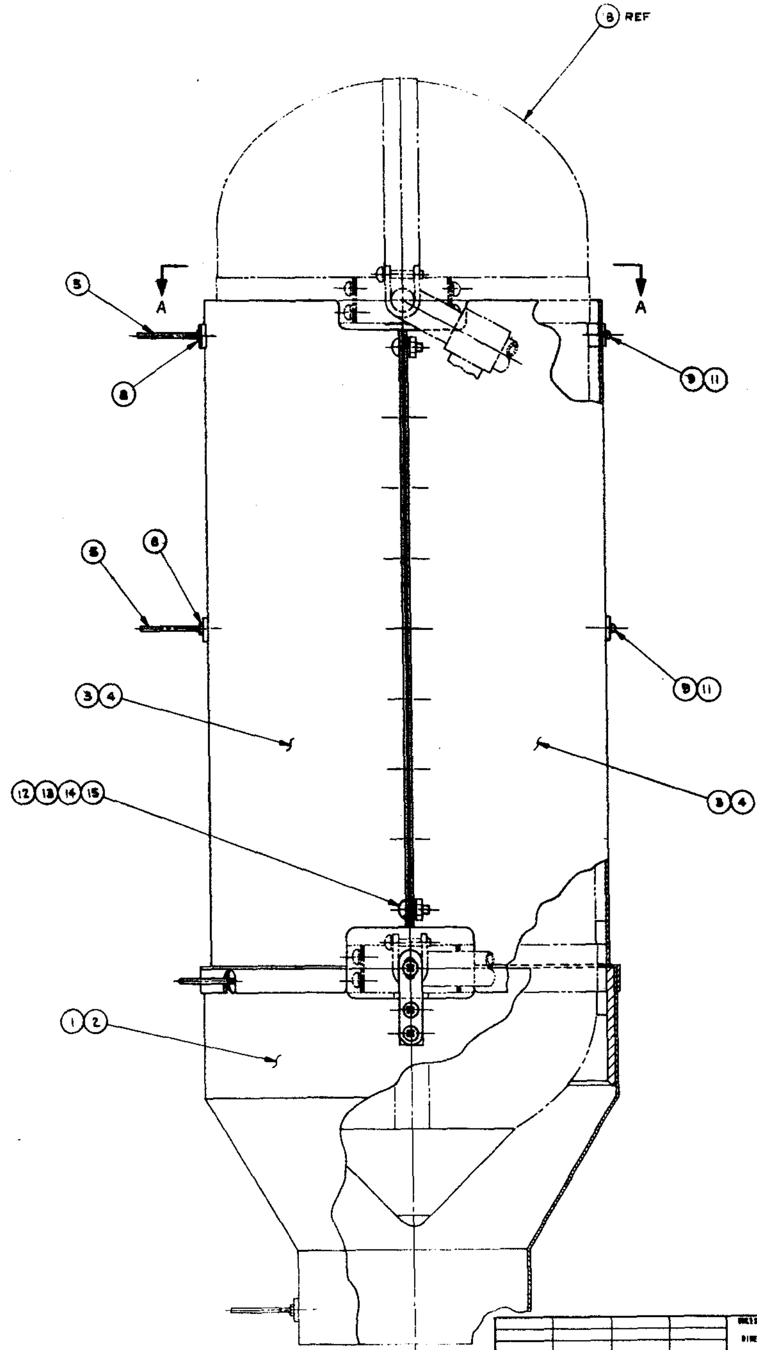

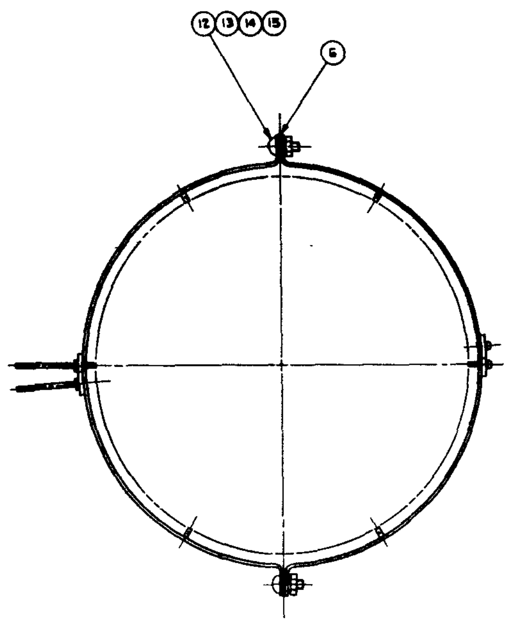

VIEW A-A

Drawing 4

QTY REQD -2	QTY REQD -1	DESCRIPTION	CODE IDENT	PART OR SPECIFICATION NO.	ITEM
					19
REF	REF	FUEL CASK MTG ASSY		2334911	18
					17
					16
18	18	WASHER, LOCK #10		MS35338-81	15
18	18	WASHER, FLAT #10		MS15795-808	14
18	18	SCREW #10-32X½		MS51958-65	13
18	18	NUT, HEX #10-32		MS35650-104	12
2	2	WASHER, LOCK #2		MS35338-77	11
					10
2	2	SCREW #2-56X⅜		MS51957-1	9
2	2	NUT, HEX #2-56		MS35649-224	8
					7
2	2	GASKET		2335340	6
2	2	TUBE, MODIFIED		2335304	5
2	—	SHROUD, HALF		2335336-10	4
—	2	SHROUD, HALF		2335336-9	3
1	—	AXIAL FLOW PURGE SYSTEM ASSY		2335095-3	2
—	1	AXIAL FLOW PURGE SYSTEM ASSY		2335095-2	1

LIST OF MATERIALS

PART NO.	NEXT ASSY	END ITEM NO.	EFFECTIVITY
2335335			MOCK-UP

DRAWING AND PART APPLICATION

DRAWING CLASS A ☐ B ☐ C ☐

FINISH

UNLESS OTHERWISE SPECIFIED:
DIMENSIONS ARE IN INCHES
TOLERANCES
DECIMAL .X ± .XX ± .XXX ±
ANGLES ±
CHAMFER ± 5°
SURFACE FINISH MICROINCHES RHR

MATERIAL:

CONTR NO. NAS-9-5829

DRAWN	R. KELLERMAN	10/11/67
CHECKED	Lewinski	9-27-67
STRESS/WT		
DSGN SUPV		
PROJ ENGR		
QUAL CONT		
SYS SPT		
DSGN APPL		
MFG		
CUSTOMER		

THE BENDIX CORPORATION
AEROSPACE SYSTEMS DIVISION – ANN ARBOR, MICHIGAN

TITLE
AXIAL FLOW
PURGE SYSTEM
WITH SHROUD

SIZE	CODE IDENT NO.	DRAWING NUMBER	REV.
E	07038	2335335	

SCALE FULL | WEIGHT | SHEET 1 OF 1

2335335

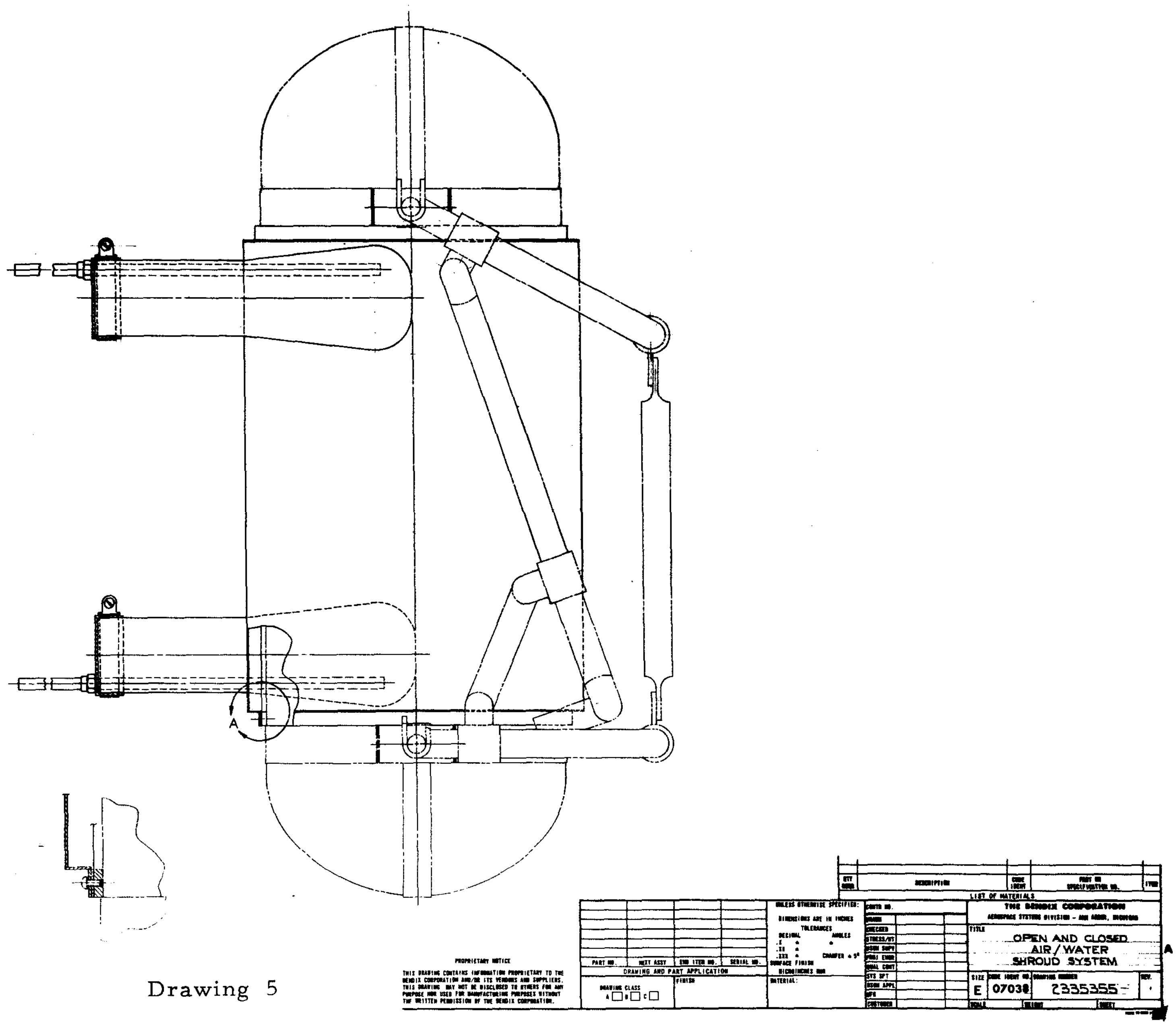
A
LIST OF MATERIALS
TITLE
OPEN AND CLOSED
AIR/WATER
SHROUD SYSTEM
SIZE
E
07038
2335355

Drawing 5

NOTES:

1. INSTRUMENTATION ON TUBELAR STRUTS TO BE LOCATED ON SIDE FACING FUEL CASK.
2. T/C'S 14, 16, 18 & 20 ON UPPER BAND.
3. T/C 15, 17, 19 & 21 ON LOWER BAND.
4. COPPER AND CONSTANTAN THERMOCOUPLE JUNCTION 24 GA. WIRE I.S.A. TYPE T.
5. EACH T/C WIRE SHOWN REPRESENTS ONE PAIR (2 WIRES).
6. ALL FINAL ASSY OPERATIONS AND INSTRUMENTATION INSTALLATION TO BE PERFORMED IN A CONTROLLED AREA AND GLOVES USED.- USE ANY OTHER NECESSARY PRECAUTIONS TO AVOID DAMAGE AND CONTAMINATION.
7. THERMOCOUPLE INSTALLATION INSTRUCTIONS:
   a. CUT TWENTY FOOT LENGTH OF WIRE AND STRIP .25 LENGTH ONE END.
   b. LOCATE T/C JUNCTION AND WELD PER BSD MP-41.
   c. STRESS RELIEVE BY WELDING NICKLE STRAPS PER MIL-W-8611 TO SUBSTRATE ONLY.
8. IDENTIFY EACH T/C WITH T/C NO SHOWN AT A POINT ONE FOOT FROM FREE WIRE END AND AT INTERVALS OF 5 FEET THEREAFTER FOR A DISTANCE OF 20 FEET.
   APPLY PROTECTIVE VARNISH COATING TO EACH MARKER
9. REFERANCE BxA DRAWING No. 2335347
10. REFERANCE BxA DRAWING No. 2335346
11. REFERANCE BxA DRAWING No 2335348
12. REFERANCE BxA DRAWING No 2335349

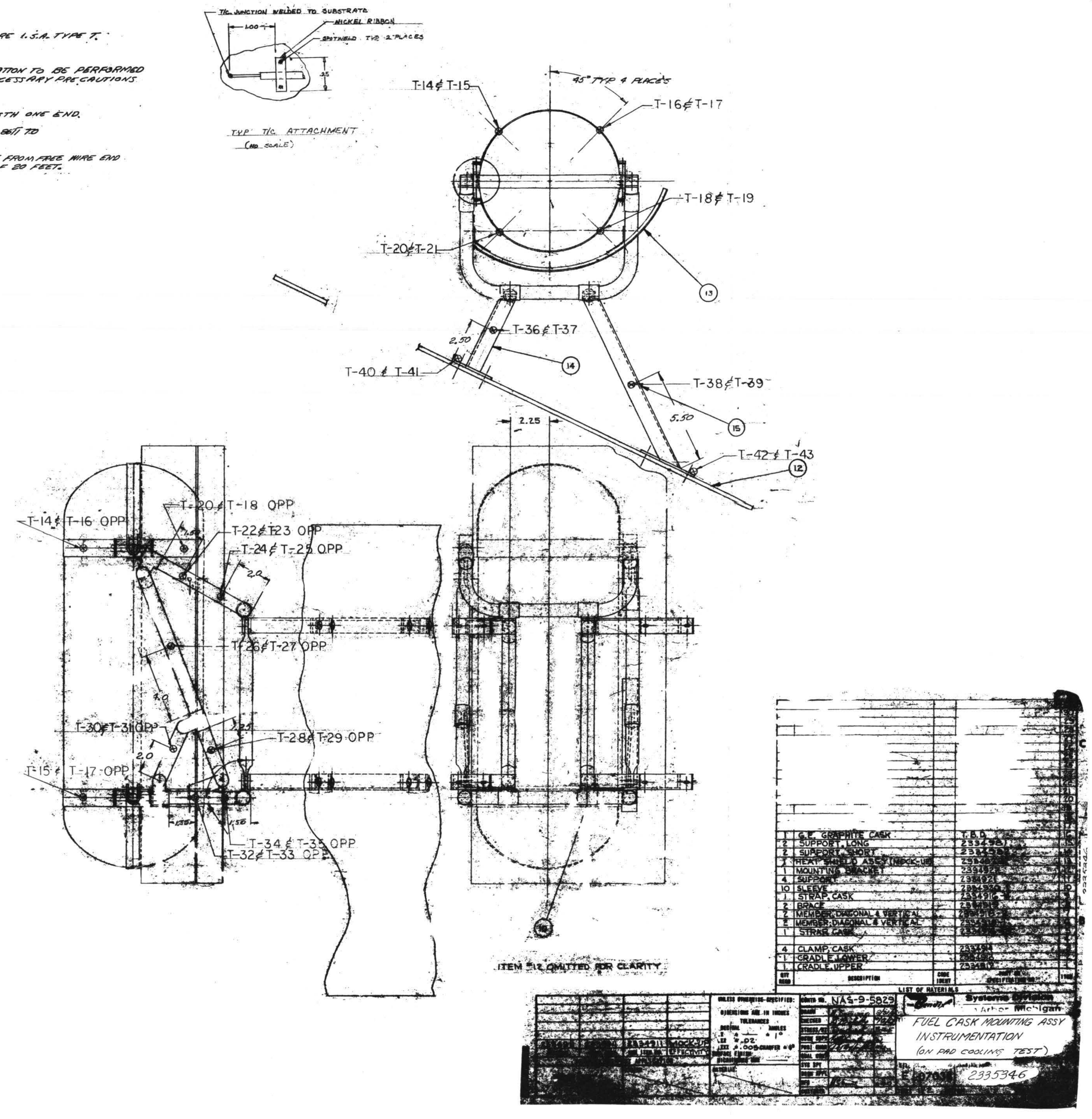

INSTRUMENTATION DESCRIPTION	INSTR. No.	DAS CHNL No.
THERMAL SHIELD	1 TO 13	
CASK SUPPORT CLAMPS	14 TO 21	
CASK SUPPORT STRUCTURE	22 TO 35	
LM SUPPORT STRUTS	36 TO 39	
LM I/F ATTACHMENT POINTS	40 TO 43	
LM VEHICAL PANEL	44 TO 53	
CASK UPPER DOME	54 TO 57	
CASK BARREL EXTERNAL SURFACE	58 TO 69	
CASK BARREL INTERNAL SURFACE	70 TO 79	
EFCS MOUNTING PLATE	80 TO 81	
EFCS SURFACE	82 TO 89	

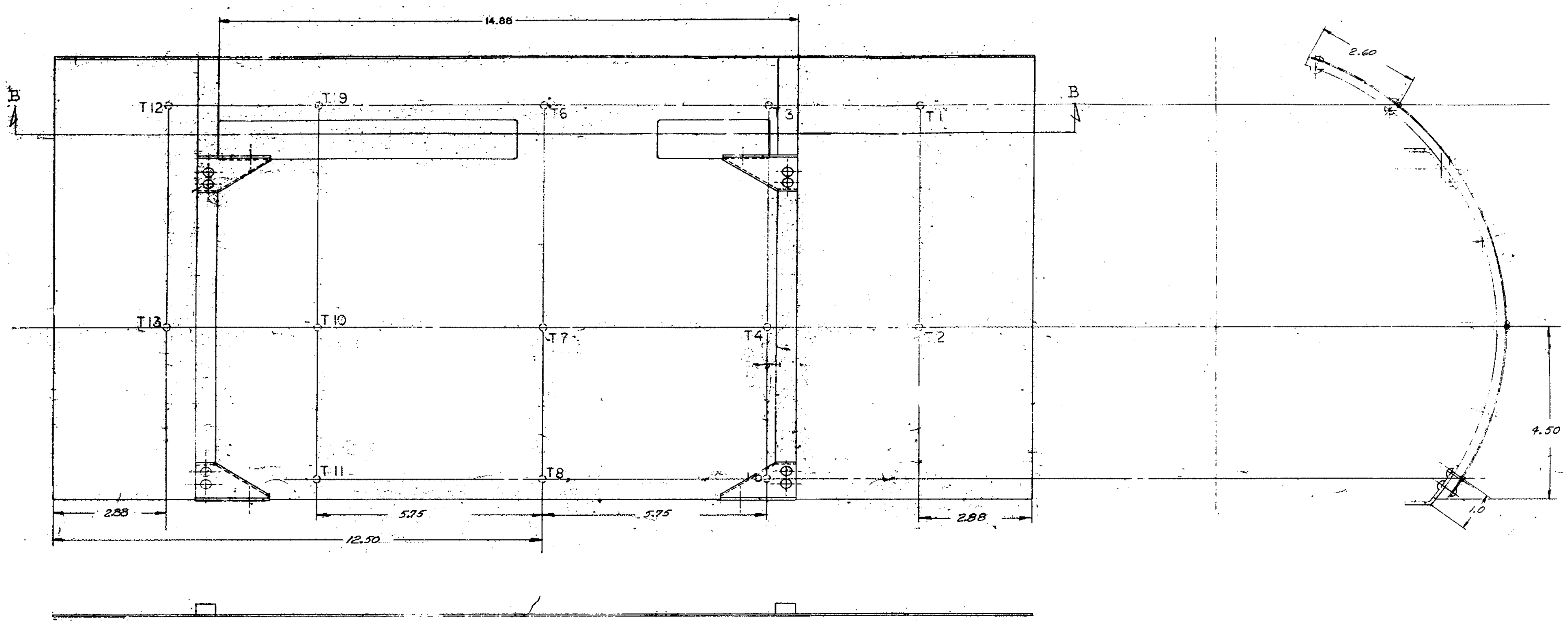

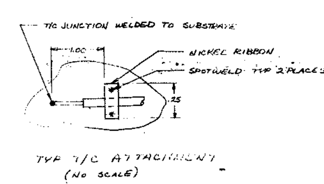

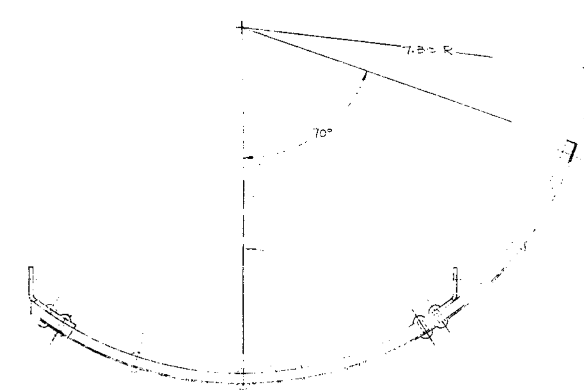

NOTES:

6. ALL T/C'S TO BE INSTALLED ON CONVEX SIDE OF THERMAL SHIELD FACING LM PANEL

5. IDENTIFY EACH T/C WITH T/C No. SHOWN AT POINT ONE FOOT FROM FREE WIRE END AND AT INTERVALS OF 5 FEET THERE AFTER FOR A DISTANCE OF 20 FEET.- APPLY PROTECTIVE VARNISH COATING TO EACH MARKER

4. THERMOCOUPLE INSTALLATION INSTRUCTIONS:
   a. CUT TWENTY FOOT LENGTH OF WIRE AND STRIP .25 LENGTH ONE END
   b. LOCATE T/C JUNCTION AND WELD PER BSD MP-41
   c. STRESS RELIEVE BY WELDING NICKEL STRAPS PER MIL-W-8611 TO SUBSTRATE ONLY

3. ALL FINAL ASSY OPERATIONS AND INSTRUMENTATION INSTALLATION TO BE PERFORMED IN A CONTROLLED AREA AND GLOVES USED.- USE ANY OTHER NECESSARY PRECAUTIONS TO AVOID DAMAGE AND CONTAMINATION

2. EACH T/C WIRE SHOWN REPRESENTS ONE PAIR (2 WIRES) COPPER AND CONSTANTAN THERMOCOUPLE JUNCTION 24 GA WIRE ISA TYPE T

QTY REQD	DESCRIPTION	CODE IDENT	PART OR SPECIFICATION NO.	ITEM
1	HEAT SHIELD ASSY		2334923	1

LIST OF MATERIALS

UNLESS OTHERWISE SPECIFIED:
DIMENSIONS ARE IN INCHES
TOLERANCES
DECIMAL .X ± / .XX ± .020 / .XXX ± .005
ANGLES ± 1°
CHAMFER ± 5°
[illegible] FINISH
[illegible]
MATERIAL
NOTED
[illegible] B.N.

CONTR NO. NAS 9-5829
DRAWN [illegible]
CHECKED [illegible] 10/11/67
STRESS/WT [illegible]
DSGN SUPV [illegible]
PROJ ENGR [illegible]
QUAL CONT
SYS SUPV
DSGN APPL
MFG [illegible]
CUSTOMER

THE Bendix CORPORATION
Systems Division
Ann Arbor, Michigan

TITLE HEAT SHIELD ASSY INSTRUMENTION (ON PAD COOLING TEST)

SIZE J
CODE IDENT NO. 07038
2335347
SCALE FULL

NOTES:

1. COPPER AND CONSTANTAIN THERMOCOUPLE JUNCTION 24 GA. WIRE, I.S.A. TYPE T
2. EACH T/C WIRE SHOWN REPRESENTS ONE PAIR (2 WIRES)
3. ALL FINAL ASSY OPERATIONS AND INSTRUMENTATION INSTALLATION TO BE PERFORMED IN A CONTROLLED AREA AND GLOVES USED. - USE ANY OTHER NECESSARY PRECAUTIONS TO AVOID DAMAGE AND CONTAMINATION
4. THERMOCOUPLE INSTALLATION INSTRUCTIONS:
   a. CUT TWENTY FOOT LENGTH OF WIRE AND STRIP .25 LENGTH ONE END.
   b. LOCATE T/C JUNCTION AND WELD PER BSD MP 41
   c. STRESS RELEIVE BY WELDING NICKLE STRAPS (ITEM No. 8) PER MIL-W-8611 TO SUBSTRATE ONLY.
5. IDENTIFY EACH T/C No WITH T/C No SHOWN AT POINT ONE FOOT FROM FREE WIRE END AND AT INTERVALS OF 5 FEET THEREAFTER FOR A DISTANCE OF 20 FEET. APPLY PROTECTIVE VARNISH COATING TO EACH MARKER
6. INSTRUMENTION TO BE LOCATED ON SIDE OF MOUNTING PLATE FACING FUEL CASK ASSEMBLY
7. PAINT ALL AREA ENCLOSED BY CROSSHATCHED BORDER WITH HIGH EMITTANCE ($\epsilon \geq 0.8$) BLACK PAINT, I.E. MICOBOND OR CATALAC BLACK PER APPLICABLE B.A MP.

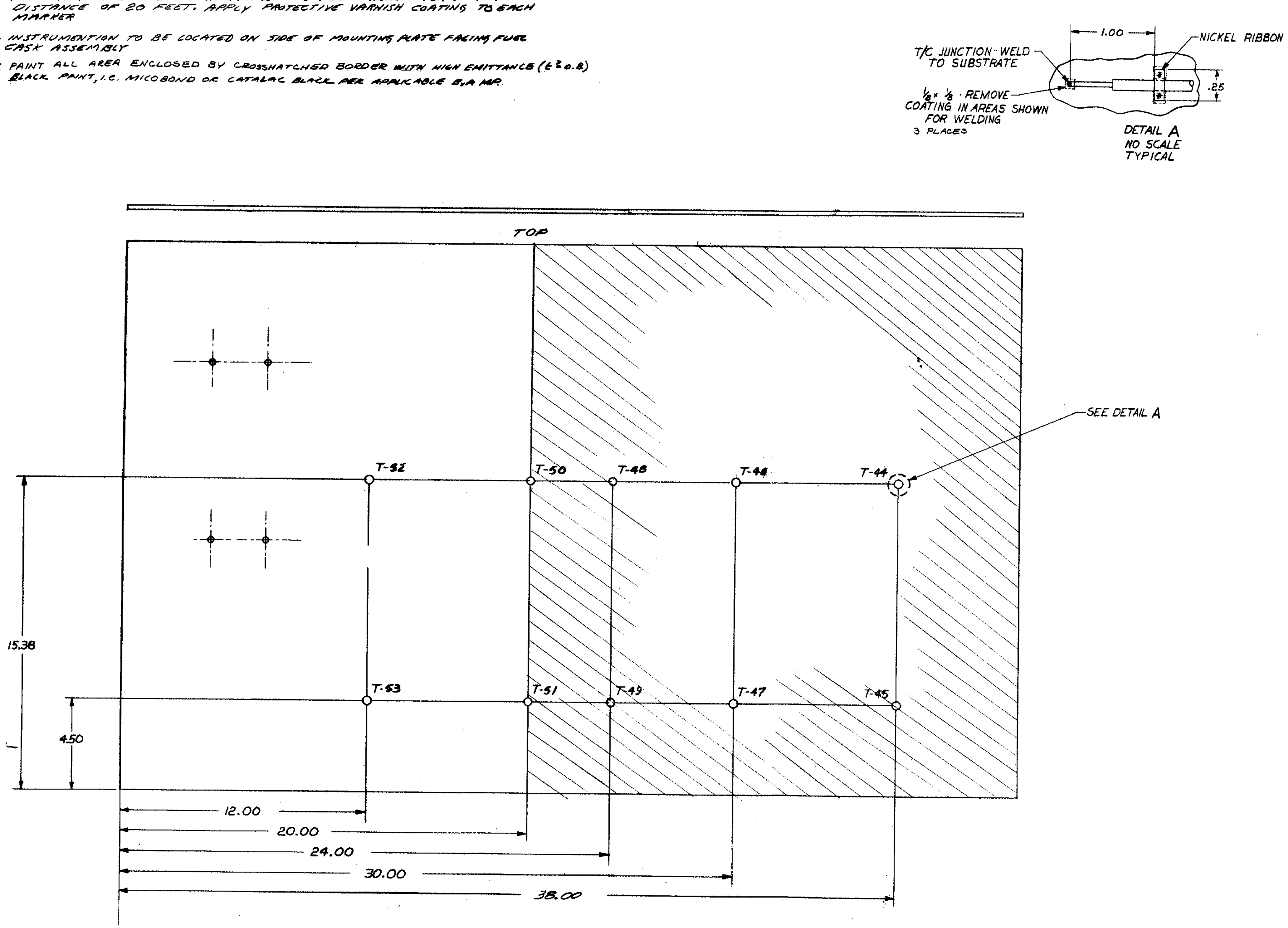

QTY REQD	DESCRIPTION	CODE IDENT	PART OR SPECIFICATION NO.	ITEM

LIST OF MATERIALS

PART NO.	NEXT ASSY	END ITEM NO.	EFFECTIVITY
2334348	—		MOCK-UP

DRAWING AND PART APPLICATION

DRAWING CLASS A ☐ B ☒ C ☐

FINISH —

UNLESS OTHERWISE SPECIFIED: DIMENSIONS ARE IN INCHES
TOLERANCES
DECIMAL .X ± — .XX ± — .XXX ± —
ANGLES ± —
CHAMFER ± 5°
SURFACE FINISH MICROINCHES RHR
MATERIAL: —

CONTR NO. NAS 9-5829
DRAWN [signature] 10/30/67
CHECKED
STRESS/WT
DSGN SUPV
PROJ ENGR
QUAL CONT
SYS SPT
DSGN APPL
MFG
CUSTOMER

THE BENDIX CORPORATION
AEROSPACE SYSTEMS DIVISION - ANN ARBOR, MICHIGAN

TITLE MOUNTING BRACKET INSTRUMENTATION (ON PAD COOLING TEST)

SIZE E | CODE IDENT NO. 07038 | DRAWING NUMBER 2334348 | REV.

SCALE 1/2 | WEIGHT | SHEET 1 OF 1

NOTES:

1. CHROMEL & ALUMEL T/C JUNCTIONS, 24 GA. WIRE
2. SPOTWELD STRESS RELIEF STRAP PER DETAIL "A" FOR MOUNTING PLATE
3. STRESS RELIEVE CAPSULE T/C'S WITH CRES SERIES 300 WIRE WOUND AROUND CAPSULE DIA.
4. ATTACH T/C'S TO GRAPHITE SURFACES PER PYROCARB 406 T/C ATTACHMENT INSTRUCTIONS
5. LOCATE & WELD T/C JUNCTIONS PER BSD-MP-91
6. T/C JUNCTION BEAD FOR INSTRUMENTATION No. T-58 THRU T-69 MUST BE A MAX OF .06 IN. DIA. TO MINIMIZE BEAD PROTRUSION FROM CASK WALL SURFACE
7. T/C LEADS T-58 THRU T-69 MUST BE ROUTED RADIALLY AWAY FROM CASK SURFACE & STRESS RELIEVED, AT FIRST RELIEF PT., A MINIMUM OF 2 INCHES FROM CASK SURFACE
8. ALL FINAL ASSY OPERATIONS AND INSTRUMENTATION INSTALLATION TO BE PERFORMED IN A CONTROLLED AREA & GLOVES USED - USE ANY OTHER NECESSARY PRECAUTIONS TO AVOID DAMAGE AND CONTAMINATION.
9. IDENTIFY EACH T/C WITH T/C No SHOWN AT A POINT ONE FOOT FROM FREE WIRE END AND AT INTERVALS OF 5 FEET THEREAFTER FOR A DISTANCE OF 20 FEET - APPLY PROTECTIVE VARNISH COATING TO EACH MARKER